Wind driven waves & re-suspension dynamics in shallow lakes: St. Lucia, South Africa

Vulindlela Zikhali

Engineering

University of KwaZulu-Natal

A thesis submitted in fulfilment of the requirements for the degree of

Master of Science

2014

Supervisor: Prof D.D. Stretch

Co-supervisor: Dr K. Tirok

For God and my loved ones

Acknowledgements

This work on wind-driven waves and re-suspension dynamics in Lake St. Lucia would not have been possible without the Ezemvelo KZN Wildlife team's contributions and assistance. The staff of the University of KwaZulu-Natal provided their expertise when it came to fabricating field equipment and the Centre for Research in Environmental, Coastal and Hydrological Engineering cannot be thanked enough. SANPAD supported this study by providing the funding without which this research would not have been possible.

I would also like to acknowledge my parents for their encouragement and God for blessing me with this opportunity. Thank you to my family and friends for the warmth, laughter and never-ending advice that accompanied every minor (and seemingly major) setback.

Finally, thank you to Dr Katrin Tirok and Prof Derek Stretch for their invaluable constructive feedback, and to my ever-enduring Nokukhanya for every big and small way she helped.

I am truly grateful to each of you.

Declaration - Plagiarism

I, Vulindlela Mcebo Sifiso Zikhali, declare that this dissertation is my own work and where use has been made of the work of others, it has been duly acknowledged in the text. This dissertation has not been submitted in partial or full to any other University. This research was carried out in my capacity as part of the Centre for Research in Environmental, Coastal and Hydrological Engineering (CRECHE), and the School of Civil Engineering. This research was conducted under the supervision of Professor D.D. Stretch and Doctor K. Tirok of the University of KwaZulu Natal, Durban.

Vulindlela Zikhali **Date**

As the candidate's supervisors, we have approved this dissertation for submission

Prof D.D. Stretch **Date**

Dr K. Tirok **Date**

Declaration - Publications

All publications presented in this work were completed and compiled by the author, Vulindlela Mcebo Sifiso Zikhali, together with Prof. Derek Stretch and Dr. Katrin Tirok who provided technical suggestions and amendments.

Published peer-reviewed journal paper

Zikhali, V., Tirok, K., Stretch, D. (2014). Wind driven waves in a shallow estuarine lake with muddy substrates: St Lucia, South Africa. Journal of Coastal Research. SI:70. 729–735.

Journal paper to be submitted for review

Zikhali, V., Tirok, K., Stretch, D. (2014). Sediment re-suspension in a shallow estuarine lake with muddy substrates: St Lucia, South Africa.

Vulindlela Zikhali **Date**

Abstract

This study investigated wind-driven wave characteristics together with associated sediment re-suspension dynamics in a shallow lake estuarine environment. Natural processes such as circulation patterns and nutrient distribution, as well as characteristics such as water quality and phytoplankton abundance depend on the physical mechanisms provided by wind-driven waves within the shallow lake habitat.

A field study was conducted over a period of 20 days wherein measuring stations were deployed throughout Lake St Lucias South Lake. Lake St Lucia is a 328 km^2 estuarine lake with a depth of $\approx$ 1 m located near the east coast of South Africa. Each measuring station consisted of a pressure transducer used to measure wave heights, and a water quality logging system to measure turbidity levels, salinity, temperature and dissolved oxygen levels. Wave stations were positioned to sample a range of fetch distances and depths as well as varying bed composition types, from areas composed of fine grained mud/silt to areas composed of large grained sand. Time series of measured significant wave heights were derived from the pressure data. Predicted significant wave heights were derived from a semi-empirical model that uses wind speed, fetch distance and average depth over fetch as input variables, but does not consider the influence of variable bed composition. The measurements were compared with the modelled significant wave heights to determine the efficacy of applying the semi-empirical wave model in an environment with variable bed composition. A simplified model relating sediment re-suspension to wave energy was also calibrated and evaluated for accuracy and efficiency using turbidity field measurements.

The wave model produced good predictions of peak significant wave heights and agreed with the observed wave development trends in conditions where the wind speed and direction were high and relatively constant respectively. Sudden wind speed and direction changes resulted in poor prediction by the model. The poor performance was ascribed to the lakes geometric complexity where slight changes in wind direction cause large changes in fetch distance; and to the models sensitivity to wind speed. Instances of wave attenuation were identified, but these cannot be conclusively linked to the effects of muddy substrates. The model for suspended sediment concentration (SSC) predicted peak re-suspension concentrations well but the settlement process was not accurately reproduced by the model. This suggests

that settling velocities may have a complex relationship to SSC, turbulence levels and suspended sediment composition.

Contents

List of Figures

List of Tables

List of Variables

a	wave amplitude
C_{10}	drag co-efficient at 10 m reference height
c	total suspended sediment concentration
c'	bed suspended sediment concentration
c_e	equilibrium re-suspended sediment concentration due to wave action
c_o	background suspended sediment concentration
c_w	wave celerity
d	average depth over fetch
E	wave energy
g	gravitational acceleration
f_p	peak frequency
H	wave height
H_c	critical wave height
H_{ref}	reference wave height
H_s	significant wave height
h	total water depth
K	modulating factor
k	wave number
L	wave length
p	pressure
SSC	suspended sediment concentration
T	wave period
U	wind speed
U_x	wind speed at fetch x
U_{10}	wind speed at 10 m reference height
u_x	friction velocity
u_b	maximum water particle horizontal velocity component
U_i	measured reference wind speed
w'	vertical fluid velocity component
w_s	settling velocity
w_o	reference settling velocity

x	fetch distance
z	reference height of measured velocity
z_o	roughness length over water
z_{ou}	upwind terrestrial roughness length
δ	dimensionless depth
δ_i	internal boundary layer height over water
ΔR	correction factor
ϵ	dimensionless energy
ρ	water density
τ	wave induced bottom stress
τ_c	critical shear stress
τ_f	reference stress
υ	dimensionless frequency
χ	dimensionless fetch
ω	angular frequency

Chapter 1

Introduction

1.1 Motivation

Wind-driven waves in shallow lakes provide the primary physical mechanisms that sustain the unique ecosystem that exists within them. Wind plays a crucial role in sustaining the hydrodynamics of shallow lakes even when they are also governed by tidal forces and river inflows. Wind activity influences nutrient release from the lake bottom, introduces circulation patterns that allow microscopic organisms to sustain, distribute and reproduce throughout the lake as well as drastically altering the physical habitat by changing water levels. Such changes can have far-reaching secondary impacts on the abundance of micro organisms and the behaviour of higher trophic levels present in the lake environment.

Lake St Lucia experiences characteristic conditions where the basic relationships between wind, wave development, sediment re-suspension and biological processes may be investigated. Similar studies have been carried out in other systems throughout the world and the lake's status as a World Heritage Site provides sufficient motivation for understanding the fundamental physical mechanisms that sustain it. The lake is a relatively undisturbed estuarine environment where the effects of anthropogenic and other external influencing factors are largely restricted. This affords us the opportunity to test the effectiveness of a widely used simple semi-empirical wave prediction model, the Young & Verhagen (1996) model, in a lake environment with a spatially varied substrate composition. The depth-averaged suspended sediment concentration (SSC) Luettich *et al.* (1990) model is also applied to determine whether the wave prediction model can be used as an input to accurately predict turbidity levels.

This research may be applied to similar shallow lake systems around the world due to the simplistic approach chosen to model the case site's governing dynamics. We were able to ascertain the effectiveness of available research methods involving wind, wave and turbidity measurement. Simple modelling equations and well-known assessment procedures were applied allowing us to reach conclusions that will support similar future endeavours.

1.2 Study Site

St Lucia is a World Heritage Site and a RAMSAR wetland of international importance. Lake St Lucia is situated near the eastern coast of South Africa in northern KwaZulu-natal. The lake may be geographically located by the coordinates $28^o00'25.96''$S, $32^o28'50.58''$E (Google Earth^{TM}, 2014). The St Lucia lake system comprises three interconnected basins False Bay, North Lake and South Lake that are linked to the sea via a 22 km long sinuous channel called the Narrows. The inlet to the system from the sea can close for prolonged periods of time due to near-shore littoral transport processes (Lawrie & Stretch, 2011a,b) and is often called the estuary of the lake although the lake as a whole is also termed an estuarine environment. Tidal effects are present for about 14 km up the Narrows when the inlet is open however the lake itself is not tidal. The inlet remained closed for the period of this study.

Lake St Lucia has a surface area of approximately 328 km^2 and an average depth of 1.0 m when the inlet is open and water levels are near the estuary mean water level (EMWL), which is a datum that is 0.25 m above sea level. When the inlet is closed the water level can differ strongly from EMWL depending on rainfall, river inflow and evaporation. South Lake has a surface area of approximately 30 km^2, extending approximately 6 km from north to south and 5 km east to west. The wind climate is characterised by prevailing north-easterly and south-westerly winds, with north-east winds dominant in the summer (Perissinotto *et al.*, 2013). The field trips discussed in this study were conducted in the lower part of Lake St Lucia, South Lake in April and July 2013 and January 2014 (see Figure 1.1).

1.3 Research Questions

The following research questions were addressed in this study:

- What are the factors affecting wave development in the simple shallow lake estuarine environment of Lake St Lucia South Lake?
- Can the wave spectrum of a shallow lake with variable substrate composition be simulated using a simple semi-empirical wave model?
- Can a simple semi-empirical wave model be used to identify instances of wave attenuation in a shallow lake?
- Can the sediment re-suspension and settling dynamics of a shallow lake with muddy substrate composition be modelled using a depth-averaged suspended sediment concentration model?
- What effect do wave characteristics have on the biological functioning of a shallow lake estuarine environment?

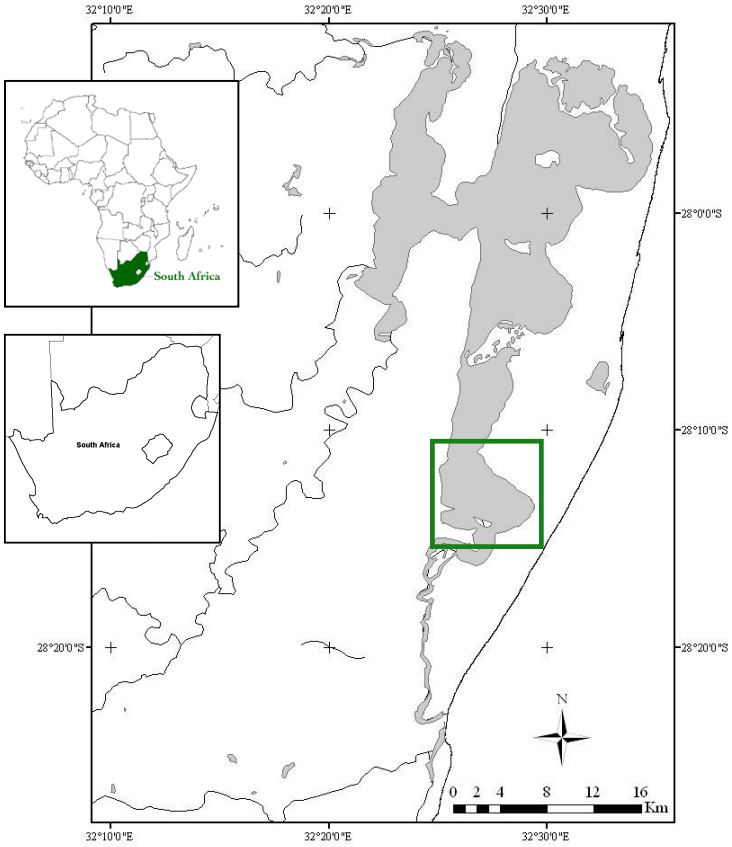

Figure 1.1: Map of Lake St Lucia where South Lake has been indicated by a green square. Adapted from Carrasco *et al.* (2013).

1.4 Aim

To measure and record wave conditions within the shallow estuarine lake of St Lucia, South Lake which has a variable substrate composition, and to apply a wave prediction model and a sediment dynamics model and assess their applicability.

1.4.1 Objectives

The objectives of the study may be summarised as follows:

1. Observe and measure the wave climate in St Lucia South Lake at locations with differing sediment substrate compositions.

2. Determine the wind climate, fetch distances and average depth over the fetch associated with the measured wave climate.

3. Apply the Young & Verhagen (1996) wave prediction model to predict the observed wave climate and determine whether wave attenuation effects exist.

4. Assess the performance of the Young & Verhagen (1996) model in terms of its ability to correctly predict significant wave heights in the St Lucia South Lake.

5. Observe and measure the turbidity levels at locations with differing sediment substrate compositions and convert these levels into SSC.

6. Apply the Luettich *et al.* (1990) SSC model using the observed waves to calibrate the model

7. Validate the SSC model by using the wave prediction model results

8. Determine the general applicability of the results derived and the boundary application conditions.

1.5 Dissertation Outline

This dissertation begins with a literature review followed by two chapters adapted from papers which address the Research Questions defined above. These papers have been adapted from their published form to fit the dissertation format. The remaining two chapters provide a summary and error analysis of the study's findings. The outline of the dissertation is as follows:

Chapter 2 provides a Literature Review where work on wave analysis and prediction studies in similar environments is discussed. Studies on sediment re-suspension dynamics are also discussed. An introduction to the relevant concepts discussed in the subsequent chapters is given and comparisons of different methods available for the study are made.

Chapter 3 consists of the paper titled 'Wind-driven waves in a shallow estuarine lake with muddy substrates: St Lucia, South Africa', co-authored by Dr K. Tirok and Prof. D.D. Stretch. The original paper is published in the Journal of Coastal Research. SI:70. 729–735. This paper discusses the field study, data analysis, Young & Verhagen (1996) model application and assessment related to investigating wind-driven wave dynamics in the South Lake of Lake St Lucia.

Chapter 4 consists of the paper titled 'Sediment re-suspension in a shallow estuarine lake with muddy substrates: St Lucia, South Africa', co-authored by Dr K. Tirok and Prof. D.D. Stretch. The original paper is to be submitted for review. Here we link the results of the wave measurement study to turbidity measurements in St Lucia South Lake. The Luettich *et al.* (1990) SSC prediction model is

applied in areas with differing benthic sediment compositions. The results of this application are discussed.

Chapter 5 is a Synthesis of the results of the previous two chapters. This chapter provides a consolidated discussion of the results derived. The applicability and shortcomings of the study are discussed.

Chapter 6 is the Conclusions and Recommendations. Here conclusions are summarised and discussed. The study is assessed with regards to the achievement of its aim and recommendations are made regarding improvements that could be made, deficiencies in the study and future investigations that could be based on this study.

References

Carrasco, N.K., Perissinotto, R., Jones, S. (2013). Turbidity effects on feeding and mortality of the copepod Acartiella natalensis (Connell and Grindley, 1974) in the St Lucia Estuary, South Africa. Journal of Experimental Marine Biology and Ecology. 446. 45–51.

Lawrie, R. & Stretch,D.D. (2011a). Occurrance and persistence of water level/salinity states and the ecological impacts for St Lucia estuarine lake, South Africa. Estuarine, Coastal and Shelf Science, 95, 67–76.

Lawrie, R. & Stretch,D.D. (2011b). Anthropogenic impacts on the water and salinity budgets of St Lucia estuarine lake in South Africa. Estuarine Coastal and Shelf Science, 93, 58–67.

Luettich, R.A., Harleman, D.R.F., Somlydody, L. (1990). Dynamic behaviour of suspended sediment concentration in a shallow lake perturbed by episodic wind events. 35. 1050–1067

Perissinotto, R., Stretch, D. & Taylor, R. (2013). Ecology and conservation of estuarine ecosystems: Lake St Lucia as a global model. New York: Cambridge University Press.

Young, I. & Verhagen, L. (1996). The growth of fetch-limited waves in water of finite depth. Part 1: The total energy and peak frequency. Coastal Enineering, 29, 57–48.

Chapter 2

Literature Review: Wind-driven waves and re-suspension dynamics

2.1 Wave description and classification

Wind driven waves form due to an interaction between wind and a body of water resulting in a physical disturbance. The wind imparts energy into the water resulting in two identifiable categories of surface waves: gravity waves and capillary waves. Gravity waves' principle maintaining force is gravity while capillary waves' principle maintaining force is surface tension (Holthuijsen, 2007). Gravity waves develop wavelengths greater than 0.017 m and are of interest due to their effect on sediment re-suspension dynamics, biological functioning and circulation patterns.

Wave analysis may be simplified by observing sinusoidal monochromatic waves and their characteristics. These characteristics are shown in Figure 2.1 and include the wave height, wave amplitude, wave length and period or frequency (Holthuijsen, 2007). These characteristics define wave behaviour and development within the physical environment. A series of wind-generated waves within a shallow lake is rarely monochromatic. Instead they consist of a spectrum of the characteristics listed above due to dynamic interactions with other waves and the environment (Sherwood & Wiberg, 2008).

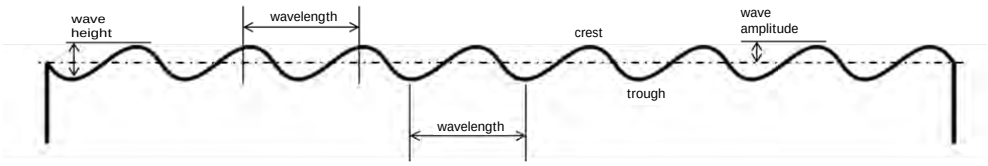

Figure 2.1: Wave characteristics

2.2 History of shallow water wave analysis

In 1925 Harold Jeffreys hypothesized that the energy within a wave developed through the interaction of air flow with the wave profile. This theory's applicability depends on the wave steepness, the ratio of wave height to the wavelength (H/L). The theory works best when describing breaking gravity waves. Additionally, the wind speed must exceed a critical value of 1 $m.s^{-1}$ and must be greater than the wave speed. The reader is referred to Kinsman (1965) and Brown *et al.* (1989) for a more detailed discussion.

Experimental studies describing shallow water wave growth were first conducted by (Thijsse, 1948). Bretschneider (1952) proceeded to identify depth limited wave growth asymptotes for wind waves in Lake Okeechobee, Florida. This work expanded on the semi-empirical wind-wave equations derived by Sverdrup & Munk (1947) and formulated the Sverdrup-Munk-Bretschneider (SMB) method. The U.S. Army Corps of Engineers also conducted field research on wave development in Lake Okeechobee (Farrer (1957), Ijima & Tang (1966), Young & Verhagen (1996) and Young (1997)). Young & Verhagen (1996) went on to expand on these experiments by investigating wave growth in depth-limited conditions in Lake George, Australia.

2.3 Wave development

Gravity waves develop when a wind greater than 1 $m.s^{-1}$ imparts enough energy into a water medium for the wavelength to become greater than approximately 0.017 m. If wind of sufficient magnitude acts on a water surface a frictional stress develops between the two fluids resulting in a transfer of energy from the less dense wind to the water. Surface waves occur at the interface between two fluids moving at different relative speeds (Brown *et al.*, 1989). This energy transfer moves through the water column causing water particles to move in an orbital to elliptical motion observed on the water surface as waves.

When water depth is much greater than the wavelength water particle motion is circular near the water surface and becomes increasingly diminished with depth (Holthuijsen, 2007; Kinsman, 1965). The radii of these water particles' circular motion is inversely proportional to the water depth. Beyond a depth of approximately half the wavelength, this circular motion is considered negligible as the particle energy has attenuated significantly with depth(see Figure 2.2) Maximum particle displacement is observed near the surface and minimum displacement at one half wavelength below the surface.

When water depth is less than or equal to half the wavelength water particle motion remains circular near the surface but becomes steadily elliptical and eventually a back-and-forth motion near the water bottom (Brown *et al.*, 1989). These limited depth conditions result in interaction between the water bottom and developing waves. Waves may either increase in height due to shoaling or decrease in height due to friction-induced attenuation. In either case further wave development due to wind becomes steadily more limited by shallow depth with increasing fetch. This condition progresses

until wave energy is no longer defined by fetch distance, instead wave energy is limited by water depth.

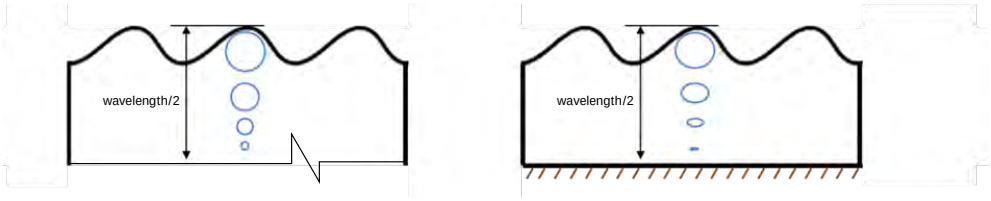

Figure 2.2: A longitudinal section of a wave field with water particle motion where the left diagram shows unlimited depth conditions and the right diagram depicts limited depth conditions

Waves are able to continue to grow in height, wavelength and speed as long as wind speed is high enough. This growth is at first rapid but eventually becomes limited by the following environmental factors:

1. Wind energy causes a tangential force to develop causing water particles to move parallel to the water surface. As a result surface currents develop, dissipating the circular motion of wave water particles (Brown *et al.*, 1989).

2. When waves become too steep due to wind-driven wave growth or the shoaling effect energy is lost due to wave breaking. If the crest gains enough momentum it overtakes the wave trunk and the wave breaks causing energy dissipation. (Brown *et al.*, 1989).

3. Wind energy is dissipated as heat by friction that develops between the moving air and water. Turbulent eddies then develop in the sheltered region of the waves and further disturb wave growth. Friction also develops between moving water particles (Brown *et al.*, 1989).

4. Non-linear wave-wave interaction due to winds of varying intensity blowing in a single direction. This produces waves of varying wavelength which interact as wave groups moving in the same direction. Spectral energy is distributed towards higher and lower frequency waves, resulting in higher energy loss occurring in the higher frequency waves (Brown *et al.*, 1989; Hasselmann *et al.*, 1973).

5. In fetch-limited conditions, where the wave form has yet to stabilize, non-linear interactions dominate developing wave groups. Lower wavelength waves break quickly as they overshoot the wave height they will assume once they stable. This results in the higher frequency, lower wavelength waves transferring their energy to longer wavelength counterparts. At the same time longer wavelength waves have yet to fully develop high/low enough crests/troughs to benefit from interaction with the wind (Kinsman, 1965).

6. In depth-limited conditions water particle orbits become more elliptical with depth until they become to-and-fro movements near the water bottom. There, wave energy decays due to shear interactions with the bottom. Furthermore re-suspended sediment in the water column attenuates wave development when a fluid mud layer develops (Brown *et al.*, 1989; Young & Verhagen, 1996; Sherwood & Wiberg, 2008).

Interference with the water bottom results in wave shoaling which increases wave height, and wave attenuation which decreases wave height. For wave shoaling transformation is dictated by the slope of the bottom and the wavelength (Kinsman, 1965). When analysing waves with a small wavelength in a shallow lake with a gradual change in slope shoaling effects may be ignored provided this analysis does not extend into regions near the lake shore (where shoaling is likely more pronounced). In the deeper parts of the lake which make up its majority wave attenuation is likely the more pronounced effect.

2.4 Wave measurement

Various methods ranging in form and function exist for measuring waves in the field. These range from instruments which convert changes in the wave field into electrical signals, to audio visual equipment used to capture wave field changes. The choice of equipment depends on the wave characteristics to be measured, the degree of accuracy required and cost allowances (Holthuijsen, 2007).

The group of available methods may be divided into in-situ and remote sensing techniques. A list of the in-situ methods follows:

1. Acoustic Doppler current profiler (ADCP): The ADCP measures near-bed water particle orbital velocities. This motion may be measured in terms of its horizontal components allowing one to determine transverse directional properties or currents. Currents can then be used to accurately determine surface wave properties such as wave direction (Holthuijsen, 2007; Sherwood & Wiberg, 2008). ADCPs are generally unable to differentiate between atmospheric pressure fluctuations and average water level changes. This is because they must remain submerged for the period of measurement, depriving them of differential pressure measurement capabilities.

2. Pressure transducer: The pressure transducer measures hydrostatic pressure below the water surface at a set frequency. This instrument may be attached to a pole and programmed to sample pressure at a high frequency (say 4 Hz) for short bursts of time. This conserves energy while ensuring a representative sample of the wave climate is captured (e.g. 5 minute sampling periods every 15 minutes). The frequency at which the instrument samples must be calibrated so as to capture the entire wave form as it passes. A low measurement frequency may cause longer wavelength waves to be accurately captured while shorter waves are not.

The correct post-processing cut-off frequency for the data to be analysed should be identified prior to deployment. This cut-off frequency should be lower than the transducer's measurement frequency to ensure no waveforms pass without being measured. It is usually difficult to determine the wave direction using a single instrument. Therefore multiple transducers may be used to resolve the directional component. The pressure transducer sees frequent use in the field due to its relatively simple setup (Holthuijsen, 2007; Mariotti & Fagherazzi, 2012).

3. Wave buoy: A wave buoy rests at the water surface moving and measuring in all 3 dimensions according to the motion of the wave field. An accelerometer is used to measure vertical displacement of the buoy by integrating the buoy's acceleration over time. (Holthuijsen, 2007). This apparatus's relatively high cost makes it a target for theft and it is known for attracting aggressive attention from wildlife. Its size and structure can also pose a risk to vessels travelling at night (making it necessary to provide some form of warning whenever a unit is deployed).

4. Wave staff: This instrument determines the vertical position of the changing water surface by measuring the electrical resistance of the dry region of a suspended wire or by measuring changes in the wire's capacitance. For the downward motion of a wave the instrument may underestimate wave amplitudes due to the development of a thin film of water over the wire. This effect is especially observable during more violent wave conditions (Holthuijsen, 2007).

5. Inverted echo-sounder: The submerged inverted echo-sounder sends out a narrow band of sound or a ping towards the water surface at set intervals. The distance from the instrument to the water surface may be calculated based on how long it takes the reflected ping to return. The speed at which the ping travels depends on the density of the water (Holthuijsen, 2007). This equipment shares similar disadvantages with the ADCP and in areas where a layer of viscous benthic material remains suspended the instrument's functionality may be compromised due to interference.

Remote sensing techniques that are available tend to be more expensive than in-situ techniques. Instruments associated with remote sensing techniques produce data sets that cover expansive areas within a short period of time. The methods available include the use of radar, stereo-photography and altimetry (Holthuijsen, 2007).

2.5 Wave theory

2.5.1 Linear wave theory:

A pressure transducer may be submerged and attached to a pole to create a wave pole capable of measuring wave-induced pressure signals. The pressure signal produced by a passing wave is increasingly attenuated with depth. The rate of attenuation depends

on the size of the wave; high frequency, small wavelength waves are fully attenuated at lower depths than low frequency waves with larger wavelengths.

To reconstruct the observed surface wave spectrum it is necessary to correct recorded wave induced pressure signals to account for attenuation. This correction may be based on linear wave theory, also known as Airy or first-order wave theory (Chadwick *et al.*, 2004). The assumptions associated with the application of this theory are as follows (Chadwick *et al.*, 2004):

1. The fluid is assumed to be incompressible with a constant density. In estuaries a vertical salinity gradient may result in differences in density therefore this assumption should be verified.
2. Waves' primary restoring force should be gravity not viscosity, surface tension or turbulence.
3. Waves should not be breaking.
4. Waves must not be steep i.e. their height should be small relative to their wavelength (for waves that do not fall into this category there are other theories available e.g. Stokes' theory, Cnoidal and stream function (Holthuijsen, 2007).
5. Water must be deep enough not to influence wave development i.e. depth must be greater than half the wavelength of the wave.

If the waves observed are subject to these assumptions linear wave theory may be applied to correct attenuated pressure signals and yield reasonably accurate results. This method has seen frequent use in current literature (Mariotti & Fagherazzi, 2012; Sherwood & Wiberg, 2008).

The linear wave theory equation may be arranged in the following manner to determine the correction factor for the attenuated pressure signal. This form enables us to reconstruct the original surface wave pressure as long as we know the wavelength and period/frequency.

$$\frac{p}{\rho\ g} = a\ sin(kx - \omega t)\frac{cosh[k(h+z)]}{cosh\ kh} \tag{2.1}$$

where the amplitude a of a surface wave of wavelength L and period T can be related to the pressure p measured at depth z in water of total depth h (Holthuijsen, 2007). Here $k = \frac{2\pi}{L}$, $\omega = \frac{2\pi}{T}$, $L = \frac{gT^2}{2\pi} tanh\ kh$, ρ is the water density and g is acceleration due to gravity.

Care must be taken when applying a correction factor to high frequency waves which may be noise produced during the transducers operation. Correcting and amplifying signal noise will result in an inaccurate corrected time series being produced.

2.5.2 Fast Fourier Transform (FFT)

In wave analysis the Fast Fourier Transform is used to identify component frequencies and amplitudes in the form of sine and cosine waves that comprise an observed time

series. (The reader is referred to texts such as Brigham (1974)) and Bloomfield (2000) which provide further discussions of the FFT). The Fourier series is a convolution algorithm capable of approximating functions using sums of sines and cosines, similar to the Taylor Series. Compared to other methods, the Fourier series approximates functions over wide intervals while keeping the amount of error to a minimum (Weir *et al.*, 2005).

The FFT may be used to identify component frequencies of the measured raw wave signal. Linear wave theory may then be used to correct the wave-induced pressure signal recorded at a known depth for the effect of signal attenuation. A cut-off frequency should be selected from the range of frequencies identified using the FFT, where signal frequencies above the cut-off are considered to be noise and excluded from correction. Alternatively an upper limit correction factor may be selected for application as seen in the work of Mariotti & Fagherazzi (2012).

The Fast Fourier Transform (FFT) efficiently (in terms of processing resources) evaluates discrete polynomials. The FFT algorithm has seen widespread use in fields ranging from medicine to engineering (Hirji, 1997).

2.5.3 Wave modeling theory: Young and Verhagen

Waves are frequently described in terms of the energy they contain per unit area. The fetch distance over which the wave develops, average depth over the fetch and the peak wave frequency are all factors that contribute to the wave energy. Together these factors may be non-dimensionalised to compare waves developed in different regions or environments. This comparison is possible due to the similar relationships between each variable (or the self-similarity) at different scales. This method of comparison was first proposed by Kitaigorodskii (1962).

The non-dimensionalised forms of these variables are:

$$\epsilon = \frac{E\ g^2}{U^4}, \quad \delta = \frac{d\ g}{U^2}, \quad \chi = \frac{x\ g}{U^2}, \quad \upsilon = \frac{f_p\ U}{g} \tag{2.2}$$

where the terms in these equations are defined as,

ϵ	dimensionless energy (unitless)
E	wave height spectrum energy (m^2)
g	gravitational acceleration ($m.s^{-2}$)
U	wind speed ($m.s^{-1}$)
δ	dimensionless depth (unitless)
d	average depth over fetch (m)
χ	dimensionless fetch (unitless)
x	fetch distance (m)
υ	dimensionless frequency (unitless)
f_p	peak frequency (s^{-1})

The JONSWAP investigation (Hasselmann *et al.* (1973)) identified the limits to the energy that a wave can develop under conditions of a low fetch distance and high depth (or deep water conditions). These limits were confirmed by Young & Verhagen (1996) during their study:

$$\epsilon = 1.6 \times 10^{-7} \chi \tag{2.3}$$

$$\upsilon = 2.18 \chi^{-0.27} \tag{2.4}$$

The spectral energy of waves which develop under these conditions is limited by the fetch - a change in water depth will not affect the overall energy of the wave group. If the depth is greatly reduced (to within a half of the wavelength) wave development is then governed by a different physical regime.

Young & Verhagen (1996) identified the limits to energy development under conditions of high fetch and low depth (shallow water conditions). The semi-empirical equations derived were found to be experimentally consistent with the results of the Bretschneider (1958) Lake Okeechobee study:

$$\epsilon = 1.06 \times 10^{-3} \delta^{1.3} \tag{2.5}$$

$$\upsilon = 0.2 \delta^{-0.375} \tag{2.6}$$

This set of limiting equations under the aforementioned conditions results in wave energy development being restricted by the water depth.

A generalized form of these equations was defined by Young & Verhagen (1996) as:

$$\epsilon = C_0 \left[tanh(C_1 \delta^{0.75}) tanh \left(\frac{C_2 \chi^{0.57}}{tanh(C_1 \delta^{0.75})} \right) \right] \tag{2.7}$$

$$C_0 = 3.64 \times 10^{-3} \tag{2.8}$$

$$C_1 = 0.493 \tag{2.9}$$

$$C_2 = 3.13 \times 10^{-3} \tag{2.10}$$

$$\tag{2.11}$$

This equation is subject to the defined upper limit to the wave energy development under conditions of high depth and high fetch (as may be observed in a fully developed sea state with an extremely high depth). The upper limit was first defined by Pierson & Moskowitz (1964) as:

$$\epsilon = 3.64 \times 10^{-3} \tag{2.12}$$

The equations defined above do not consider the possible effect of different sediment composition on the development and dissipation of wave energy. The error analysis of the study by Young & Verhagen (1996) hints at the possibility of another variable contributing to the scatter observed in their results. Most of the scatter is explained as due to the gustiness of the wind and variability accuracy when defining the fetch distance.

Holland *et al.* (2009) observed instances of attenuated wave heights that in nearshore and muddy regions compared to offshore wave heights. These observations support the concept of significant wave attenuation effects due to muddy substrates. This attenuation goes beyond energy loss due to shoaling over sand bars as observed when a SWAN (Simulating Waves Nearshore) model was used by Cuchiara *et al.* (2009) to simulate wave energy attenuation due to fluid mud. SWAN is a wave modelling package designed to predict the wave spectrum likely to develop in shallow coastal areas using wind, current and substrate composition as inputs. The model is computationally economic relative to other spectral models when considering deep to shallow water wave propagation and dissipation effects (Alomar *et al.*, 2014). However spectral wave analysis still requires extensive processing power and time. A similar study by Mehta & Jiang (1990)) found that wave attenuation was frequency dependent with higher frequency waves being attenuated by up to 75%.

Wind correction factor

The wind boundary layer that develops over land differs from the boundary layer over water (Walmsley *et al.*, 1989). Wind speeds measured over land should be corrected for applications over sections of water. These corrections need to be applied according to the wind direction's corresponding surface roughness and the fetch distance over the water.

Young & Verhagen (1996) describe how wind moving from a land region into an open water region may be corrected by a factor ΔR, where

$$U_x = U_i + \Delta R \, U_i \tag{2.13}$$

Here U_i is the (measured) reference wind speed prior to crossing the shoreline, U_x is the wind speed at a fetch distance x downwind from the shoreline crossing point, and ΔR is a correction given by

$$\Delta R = \begin{cases} \frac{ln(\frac{z}{z_0}) \; ln(\frac{\delta_i}{z_{ou}})}{ln(\frac{z}{z_{0u}} \; ln(\frac{\delta_i}{z_0}))} - 1 & , \text{for } z \leq \delta_i \\ 0 & , \text{for } z \geq \delta_i \end{cases} \tag{2.14}$$

Here z is the reference height of the velocity, z_0 is the roughness length over water, z_{0u} is the upwind terrestrial roughness length, and δ_i is the internal boundary layer height over water given by

$$\delta_i = 0.75 z_0 \left(\frac{x}{z_0} \right)^{0.8} \tag{2.15}$$

The roughness length over the water z_0 is assumed to vary with wind speed (Young & Verhagen, 1996) as described by

$$z_0 = A\frac{u_*^2}{g} \tag{2.16}$$

$$u_*^2 = C_{10}U_{10}^2 \tag{2.17}$$

$$C_{10} = (0.8 + 0.065U_{10}) \times 10^{-3} \tag{2.18}$$

Where A=0.0185, u_* (m.s^{-1}) is the friction velocity, U_{10} (m.s^{-1}) is the wind speed at a reference height of 10 m, and C_{10} is a drag co-efficient.

2.6 Wind waves statistical analysis

The significant wave height is a value defined as the average of the top one-third of the wave heights of the wave record (Holthuijsen, 2007). This representative wave height is used to assess the wave energy and wave climate in engineering design and wave analysis. The statistically determined definition $H_s = 4\sqrt{E}$ may be used to calculate the significant wave height of waves provided their arrangement follows a Rayleigh distribution. Here E is defined as the integral of the wave height spectrum.

2.7 Summary: Wind-driven waves in shallow lakes

Hydrodynamic disturbances introduced by the wind's transmission of energy into the water attenuates with depth. At approximately half one wavelength below the water surface this disturbance may be considered negligible in terms of its hydrodynamic effects.

Shallow lake and deep water wave development are similar in that the distance of fetch and the duration of wind exposure largely determines resulting wave energy. However in shallow water depth influences wave development by limiting the energy a wave can develop. Describing a wave field begins by using available methods of measurement to collect either pressure, velocity or visual data. This data is then corrected and processed to produce information such as significant wave height, peak period or wave direction. In shallow lakes the Young & Verhagen (1996) semi-empirical equations can approximate significant wave heights using only wind magnitude, fetch distance and average depth over fetch.

2.8 Wave interaction with a shallow lake bottom

Shallow lake hydrodynamic are largely driven by wind, especially where tidal variation and river inflow effects are negligible. Waves influence mechanical processes such as sediment and microalgae re-suspension, turbidity levels and lake-wide particle circulation. These processes are fundamental to the biological and physical sustainability of shallow lake and estuarine habitats and ecologies.

Should the water depth become less than one wavelength in magnitude wave induced water particles' elliptical motion is interfered with by interaction with the benthos (see Figure 2.3). Waves in this condition are considered to be transitional or shallow water waves as opposed to deep water waves. The effect of interaction with the bottom increases with decreasing depth. In the case of wave attenuation the degree of interference is dependent on water bottom sediment composition (mainly the roughness) and wave frequency or wavelength. Waves travelling at a higher frequency are less dampened than lower frequency waves which have a larger wavelength(Mehta & Jiang, 1990). Interaction with a muddy bottom may transform the wave form in shallow lakes as well as in coastal areas where muddy deposits provide coastal protection (Holland *et al.*, 2009).

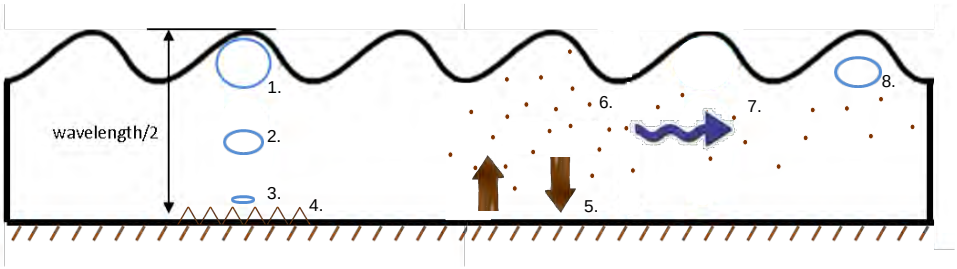

Figure 2.3: Schematic diagram of a wave interaction with a muddy bottom in a shallow lake. 1: Elliptical motion of water particles due to wind. 2: Attenuation of wave with depth and flattening elliptical motion due to interaction with bottom. 3: Nearly zero vertical fluctuation due to proximity to muddy bottom 4: Wave action shear stress loosens sediment 5: Sediment re-suspension together with settlement occurs, 6: Re-suspended sediment is distributed throughout the vertical water column due to wind-wave and wind induced current and turbulence 7: Wind-driven currents carry sediment throughout the lake 8: Elliptical motion of water particles is dampened by suspended particles and observable wave attenuation occurs

In shallow lakes the horizontal and bottom-parallel water particle motion that develops near the lake benthos defines the erosion effect on mud layers. This motion exerts a shear force which causes water particles to be entrained in the water column. The wave generated shear stress is greatest within the region closest to the lake bottom (Wiberg & Sherwood, 2008).

Bottom roughness affects the amount of sediment entrained in the water column by

influencing wave particle motion and water bottom structure interaction. A rougher surface is likely to experience more re-suspension events than a smooth surface due to increased resistance and shear force interactions (Holmedal & Myrhaug, 2000).

The direction of the current or particle motion forcing sediment re-suspension also affects the amount of sediment being re-suspended. The alignment of current movement with the water bottom surface may result in different degrees of roughness. When shear force is applied in a direction perpendicular to existing bed ripples a higher roughness value may assigned. When particle movement is parallel to bed ripples a lesser roughness value is appropriate due to a lesser resistance. The increased roughness leads to increased turbulence in the region near the lake bed (Holmedal & Myrhaug, 2000).

Suspended sediment found in rivers and shallow lakes is likely to have been loosened by turbulent flows due to tides, wind-driven currents or waves before being distributed throughout the lake by advective currents (Brand *et al.*, 2010). In many shallow lakes tidal variation in water levels results in the development of horizontal currents. In lakes without a significant tidal range sediment transport is controlled by wind-driven waves and currents. Waves provide the shear energy necessary for re-suspension while currents drive sediment transport from one part of the lake to another. This interaction with the rough bottom boundary and the internal friction that develops while keeping particles in suspension results in energy loss to the waves and observable wave damping (Holland *et al.*, 2009).

Entrained sediment particles make a significant contribution to the total sediment transport observed throughout shallow lakes. Even in the absence of significant advective currents some re-suspended sediment is kept entrained by wave-induced elliptical motion. At the same time other particles settle through the water column back to the bottom depending on their size, the water's chemical properties and the sediment's composition (Maine, 2011).

2.9 Turbidity measurement

Turbidity may be defined as the decrease in the clarity of a solution due to the presence of suspended material which may be organic or inorganic in nature (Tananaev & Debolskiy, 2014). Turbidity measurement usually involves using an instrument to measure the amount of scattered, reflected or attenuated light shone through a fluid medium to determine the number of entrained particles. The higher the intensity of the affected scattered light or the lower the intensity of the unaffected light, the higher the turbidity (Ziegler, 2002). This process is a form of optical measurement and is applied using laser diffraction. Optical gauges are especially suited for measuring concentration ranges of 0-1000 mg.ℓ^{-1} although higher concentrations can be measured (Foster *et al.*, 1992).

Turbidity is usually measured in nephelometric turbidity units (NTU). Other devices used include ultrasonic and nuclear scattering gauges. Turbidity is a function of particle size, shape, density, composition and water colour (Tananaev & Debolskiy,

2014; Foster *et al.*, 1992; Rügner *et al.*, 2014; Ziegler, 2002). The colour of blacker or darker sediment is known to affect optical backscatter meters by causing a negative bias in measurements (light may be absorbed by these particles causing under-prediction of turbidity) (Ziegler, 2002). Samples that contain organic matter such as phytoplankton or macrophytes may undergo a change in the amount of suspended sediment and/or turbidity if stored for periods of time. The organic matter may grow and affect subsequent turbidity readings unless precautionary measures are applied.

The vertical position of the optical backscatter meter within the water column may also affect the measured turbidity level if it is incorrectly assumed that the sediment concentration is the same throughout the water column.

To correlate the SSC in the water column against measured NTU a calibration regression curve must be constructed. This curve relates the amount of suspended sediment to the turbidity of the water where SSC is determined using the dried residue from membrane filtered water samples (Brand *et al.*, 2010; Rügner *et al.*, 2014). To interpret turbidity results a relationship between the turbidity levels measured and the type of sediment present in the area must be established as the shape, size and density of the particle may affect the turbidity reading. The relationship between SSC and turbidity may be described as either linear, power law or polynomial. A study by Tananaev & Debolskiy (2014) demonstrates how the accuracy of the derived regression relationship may be further improved by correcting for background optical properties of the water sample. This would lead to a suspended sediment correlation curve described as:

$$SSC = M(T - T_f) + N \tag{2.19}$$

Here M and N are constants, T is turbidity and T_f is the filtered sample's residual turbidity value. This residual turbidity is due to water colour.

In their bivariate calibration the R^2 correlation is observed to improve by 0.03 and RMSE is reduced by just under 0.5 units. This marginal improvement would be more pronounced where specific measurement of SSC levels is important and water colour is more influential. A simplified model of re-suspension in shallow lakes would benefit from this improved accuracy depending on the site specific water properties.

The SSC to turbidity relationship may also reach an upper saturation point at high turbidity levels. Beyond this point large changes in NTU will result in only a small change in SSC (Tananaev & Debolskiy, 2014).

2.10 Benthic sediment composition and SSC

Cyclic loading on the water bottom caused by wave action together with a build-up of excess pore pressure can cause the bottom to fluidize and form a lutocline Mehta & Jiang (1990). When the cohesive inter-particle bonds that form the structural matrix of the bottom layers are broken down a loose mud layer may persist until such wave action ceases and sedimentation is allowed to occur. The persistence of this layer is caused by the bed erosion flux exceeding the near-bed upward entrainment flux (Ross

& Mehta, 1989) This fluidized state increases the likelihood of sediment becoming re-suspended into the water column, due to either wave action or currents. The fluidized mud offers less resistance to shear forces due to a lower critical shear strength τ_c. Therefore the growth and persistence of fluid mud layers and lutoclines in shallow lakes has a significant impact on horizontal sediment transport rates (Ross & Mehta, 1989).

A lutocline may be described as a horizontal fluid mud layer consisting of a sharp sediment concentration gradient (Ross & Mehta, 1989). Typically this layer is positioned above a cohesive bed and below a mobile suspension layer (see Figure 2.4). The range of sediment concentrations in the mobile suspension layer is usually below 1000mg.ℓ^{-1} but this may increase during storm events. While local regions with high concentration gradients may develop within this layer (Ross & Mehta, 1989) in shallow lakes it is acceptable to assume turbulent mixing that results in a fairly uniform concentration with depth (Bailey & Hamilton, 1997; Luettich *et al.*, 1990). The formation of a lutocline may dampen waves, especially those waves with a longer wavelength. Lutoclines also decrease the total energy available for re-suspension of sediment particles which may ultimately result in less turbid water.

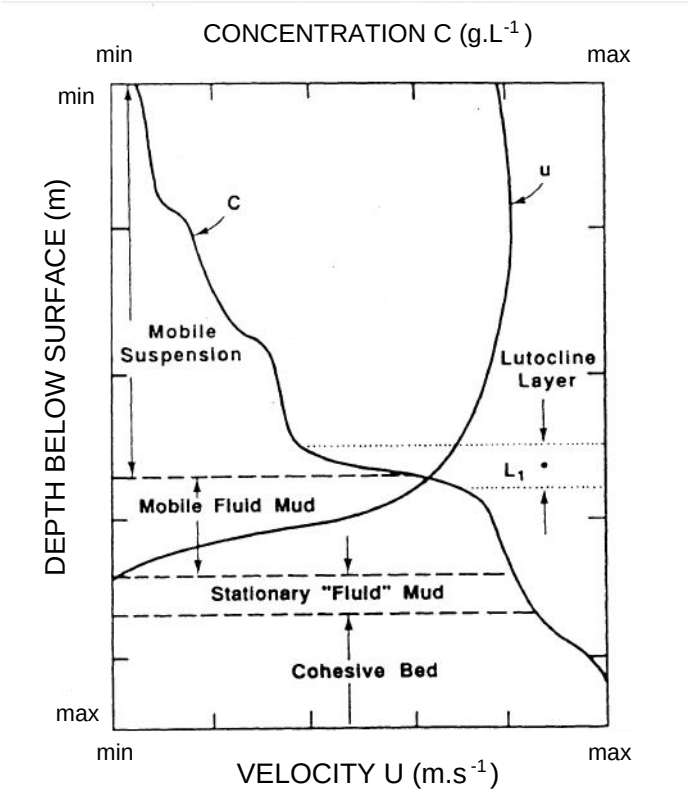

Figure 2.4: Schematic diagram of a sediment concentration and velocity profile. Adapted from Ross & Mehta (1989)

The geological state of the area where re-suspension occurs may also have a significant impact on the degree of SSC. Compacted or consolidated water bottoms offer a higher resistance than looser, less consolidated materials (Ross & Mehta, 1989). Heavier sediment requires more wave energy to be mobilised therefore the water column above a benthic region comprising of higher density sand particles may remain less turbid under wave action.

However geometrically larger grain sizes may not necessarily be heavier or denser. This is especially likely when observing a clay or silt-dominated suspended sediment solution where flocs are likely to form. Flocs may be described as electro-chemically linked clay particles which form structures that are large compared to singular suspended sediment forms(Maine, 2011).

2.11 Modelling re-suspension dynamics

In shallow lakes wave-generated bottom stresses have a greater impact on the re-suspension of sediment than those stresses generated by currents (Bailey & Hamilton, 1997). One way of modelling suspended sediment concentration (SSC) is to directly model the rate of change in concentration with time in an empirical manner. This method is based on observations made of the suspended sediment's re-suspension and deposition flux. This method allows one to circumvent the difficulties associated with parametrizing physical processes.

Another way of modelling suspended sediment concentration (SSC) involves modelling the rate of change in concentration levels (Luettich *et al.*, 1990). This method is more physically correct and allows for more general application than the purely empirical method. In shallow lakes vertical mixing due to turbulent forces created by wind-driven waves can cause the sediment concentration to be the same throughout the vertical water column (Bailey & Hamilton, 1997; Luettich *et al.*, 1990). Depth-averaged suspended sediment prediction models are therefore effective when applied to most shallow lakes. The method of modelling the rate of change in concentration levels will be discussed in the following paragraphs.

Sediment concentration flux may be represented by an equation expressing the sediment mass transport balance. If the molecular diffusion and horizontal advection terms are less significant than the turbulent forces the transport balance may be described as

$$\frac{\partial c}{\partial t} = -\frac{\partial}{\partial h}(-\overline{w'c'}) - w_s \frac{\partial c}{\partial h} \tag{2.20}$$

where c is the total suspended sediment concentration, c' is sediment released from the bed. h is the total depth, w' is the vertical velocity component and w_s is the settling velocity (here movement upwards is the considered positive) (Brand *et al.* (2010); Luettich *et al.* (1990)). Changes in SSC are therefore simply the amount of sediment added to the vertical column (first term) less the amount of sediment that settles out (second term). The amount of sediment re-suspended is a function of the fluid velocity's vertical component which is determined by waves or current. The amount of sediment returned to the bed depends on particle settling velocity.

To obtain the depth averaged total amount of sediment available in the water column we integrate the flux equation over the depth assuming constant depth and no flux across the free surface:

$$h\,\frac{\delta \overline{c}}{\delta t} = \Phi \tag{2.21}$$

where

$$\overline{c} = \frac{1}{h}\int_{-h}^{0} c\,\mathrm{d}z \tag{2.22}$$

$$\Phi = -w_s c_{fact}|_{-h} + \overline{w'c'}|_{-h} \tag{2.23}$$

where c_{fact} is a factor related to the distribution of suspended sediment concentration over the depth. If this distribution is uniform c_{fact} is equal to 1.

Sediment re-suspension and transferral into the water column is dependent on the bottom shear stress and its relation to a critical shear stress. The critical shear stress approximates the benthic structure's physical resistance which must be exceeded for re-suspension to occur.

A parametrization of equation 2.21 would be

$$\beta \equiv \frac{-w_s c_{fact}|_{-h}}{c} \tag{2.24}$$

and

$$c_e \equiv \overline{w'c'}|_{-h} \tag{2.25}$$

which allows us to define equation 2.21 as

$$h\,\frac{d\overline{c}}{dt} = -\beta\ c + c_e \tag{2.26}$$

The parametrization of β suggests that downward sediment flux due to settling is equal to the settling velocity multiplied by a factor that is defined by the distribution of suspended sediment within the water column. If there is no significant suspended sediment gradient in the vertical direction then $\beta \approx w_s$.

Sediment re-suspension c_e is a function of excess wave-induced bottom stress where,

$$c_e = \begin{cases} c_o + K\left(\frac{\tau_{bw}-\tau_c}{\tau_{ref}}\right)^n & \text{for } H_s > H_c \\ c_o & \text{for } H_s < H_c \end{cases} \tag{2.27}$$

The term c_e describes the equilibrium sediment concentration driven by wave action. During calm wave periods of the field study conducted by Luettich *et al.* (1990) the suspended sediment concentration was seen to remain above a certain value. This sediment concentration was identified as the background concentration c_o of the lake water. This background concentration was explained as due to the presence of small inorganic particles and organic particles which were in a state of major bloom during the period of investigation. This factor must be considered when determining the total

suspended sediment in the water column. The variable K acts as a modulating factor with units of mg.ℓ^{-1}. The parameter τ is the wave induced bottom stress, τ_c is a critical shear stress which regulates when re-suspension occurs while τ_{ref} is a reference stress equal to 1 and serves to make the term in parenthesis dimensionless and n is an exponential term. The value of n may be defined by the relationship between the wave induced shear stress and the mean wave induced orbital velocity at a particular depth(Wiberg & Sherwood, 2008),

$$\tau_{bw} = \frac{\rho f_w u_b^2}{2} \tag{2.28}$$

where ρ is the water density, f_w is a friction factor and u_b is the maximum velocity of a water particle observed when the vertical component is 0. The bottom shear stress is expected to scale approximately on the induced velocity squared so that a value of $n = 2$ seems appropriate. This assumption is illustrated by

$$u_b = \frac{H\pi}{Tsinh(kh)} \tag{2.29}$$

as described by Wiberg & Sherwood (2008). For $kh \ll 1$, $sinh(kh) \rightarrow kh$ therefore Equation 2.29 may be expressed as

$$u_b \approx \frac{H\pi}{T(kh)} = \frac{HL}{2Th} = c_w \frac{H}{2h} \tag{2.30}$$

Where c_w is the wave celerity. Therefore Equation 2.28 may be described as,

$$\tau_{bw} = \frac{\rho f_w}{2} \left[c_w \frac{H}{2h} \right]^2 \tag{2.31}$$

where H is the wave height. If a constant depth is assumed for the period of the wave's propagation the re-suspension term E may be described as

$$c_e = \begin{cases} c_o + K \left(\frac{H_s - H_c}{H_{ref}} \right)^2 & \text{for } H_s > H_c \\ c_o & \text{for } H_s < H_c \end{cases} \tag{2.32}$$

This description allows us to express equation 2.20 as

$$\frac{dc}{dt} = -\frac{w_s}{h} (c - c_e) \tag{2.33}$$

An analytical solution for the amount of suspended sediment concentration present in the water column may therefore be described as,

$$c(t + \Delta t) = c(t) e^{-w_s \Delta t / h} + c_e(t) \left(1 - e^{-w_s \Delta t / h} \right) \tag{2.34}$$

One shortcoming of this model is that the effects of turbulence or the consequent inertia of re-suspended particles has not been incorporated. This has been identified as

a shortcoming of many sediment re-suspension and deposition models as turbulence has a significant effect on settling rates (Bailey & Hamilton, 1997). Excluding diffusion may also adversely affect the model's accuracy. However excluding the effect of currents may be appropriate where their magnitude is low compared to waves (Bailey & Hamilton, 1997; Luettich *et al.*, 1990)

2.12 Ecological effects of turbidity levels

Water quality is affected by the amount and type of sediment suspended in the water column. Transport of nutrients together with harmful pollutants is strongly correlated with the transport and hence the re-suspension of suspended sediment (Rügner *et al.*, 2014). Suspended sediment controls the amount of light penetration through the water column and provides a means of transport for micro organisms. Lake bottom porosity and the amount of re-suspended sediment entrained in the water column affect available levels of dissolved phosphorous and nitrate. These levels can have a measurable effect on the development and sustained abundance of primary producers such as phytoplankton and macrophytes in shallow lakes (Bailey & Hamilton, 1997; Brand *et al.*, 2010; Tananaev & Debolskiy, 2014).

Changes in climate and land use can increase sediment load and re-suspended sediment levels in shallow lakes. Tirok & Scharler (2014) highlight how together with changes in water depth, turbidity levels can significantly affect the amount of light available to primary producers. Variability in depth and turbidity are seen to affect benthic and pelagic algae production differently due to resulting light penetration. For high mean turbidities a shallow depth and high variability in turbidity have a less pronounced effect on benthic biomass production than pelagic. As depth increases and turbidity variability decreases benthic production is more severely diminished while pelagic production becomes more pronounced.

High turbidity levels can adversely affect fish populations by causing acute stress responses such as increased cardiac activity, elevated plasma cortisol and changed hematological parameters (Berli *et al.*, 2014). The respiratory abilities of juvenile fish and species poorly adapted to high turbidity environments may also be adversely affected. Berli *et al.* (2014) concluded that high turbidity levels impaired the swimming ability and physiology of freshwater salmonids. Suspended sediment can provide as a protective mechanism to lower trophic level organisms against predators by obscuring visibility or affording opportunities for camouflage. Conversely, predator population may decrease due to high turbidity levels. Short term changes in turbidity levels due to storm conditions and high precipitation also affect aquatic organism routine and can cause stress responses. In Lake St Lucia variability in turbidity levels is able to reduce long term net biomass production by up to 30% as compared low variability conditions (Tirok & Scharler, 2014). This reduction was found to have the greatest potential effect at low turbidities with lesser reductions observed at higher turbidities.

Measurements of the amount of biomass and consequently the health of a lake environment also rely on turbidity. Sediment transport also heavily relies on re-suspended

sediment concentration together with current (wind induced or otherwise).

2.13 Summary: Re-suspended sediment dynamics

Suspended sediment dynamics are crucial for the ecology of shallow lakes. The process of re-suspension sustains the development of primary producers but can also adversely affect these producers and higher trophic levels of the food chain.

Re-suspension dynamics in shallow lakes are governed by wind-driven wave and current activity. In shallow lakes wind-driven waves provide the dominant energy that drives re-suspension. Various methods exist for modelling suspended sediment with suitability dependent on the hydrodynamic conditions present. Depth averaged turbidity modelling is appropriate in shallow lakes with low currents and little to no vertical suspended sediment gradient.

The Luettich *et al.* (1990) depth-averaged suspended sediment concentration equations can accurately approximate the re-suspension dynamics in shallow lakes. The model may not perform as well in conditions where considerable advective currents exist or there is a pronounced turbidity gradient.

References

Alomar, M., Sanchez-Arcilla, A., Bolanos, R., Sairouni, A. (2014). Wave growth and forecasting in variable, semi-enclosed domains. Continental Shelf Research. 87. 28–40.

Bailey, M.C. & Hamilton, D.P. (1997). Wind induced sediment resuspension: a lake-wide model. Ecological Modelling. 99. 217–228.

Berli, B.I., Gilbert, M.J.H., Ralph, A.L., Tierney, K.B., Burkhardt-Holm, P. (2014). Acute exposure to a common suspended sediment affects the swimming performance and physiology of juvenile salmonids. Comparative Biochemistry and Physiology, Part A. 176. 1–10.

Bloomfield, P. (2000). Fourier analysis of time series: an introduction. New York: John-Wiley & Sons Inc.

Brand, A., Lacy, J.R., Hsu, K., Hoover, D., Gladding, S., Stacey, M.T. (2010). Wind-enhanced resuspension in the shallow waters of South San Francisco Bay: Mechanisms and potential implications for cohesive sediment transport. 115.

Bretschneider, C. (1952). The generation and decay of wind waves in deep water. Trans. Am. Geophys. Union, 33, 381-389.

Bretschneider, C. (1958). Revised wave forecasting relationships. 6th Conference on Coastal Engineering. (pp.30-67). New York:ASCE.

Brigham, E. (1974). The Fast Fourier Transform. New Jersey: Prentice-Hall.

Brown, J., Colling, A., Park, D., Phillips, J., Rothery, D. & Wright, J. (1989). Waves, tides and shallow-water processes. Milton Keynes: The Open University

Chadwick, A., Borthwick, M., Morfett, J. (2004). Hydraulics in civil and environmental engineering. Abingdon: Spon Press.

Cuchiara, D.C., Fernandes, E.H., Strauch, J.C., Wintwerp, J.C., Calliari, L.J. (2009). Determination of the wave climate for the southern Brazilian Shelf. Continental Shelf Research, 29, 3, (pp.545-555).

Farrer, L. (1957). Wind tides on Lake Okeechobee. 6th Coastal Engnineering Conference (pp.134-146). California: Council Wave Research.

Foster, I.D.L., Millington, R., Grew, R.G. (1992). The impact of particle size controls on stream turbidity measurement; some implications for suspended sediment yield estimation. Erosion and Sediment Transport Monitoring Programmes in River Basins. Proceedings of the Oslo Symposium. 210. 51–62

Hasselmann, K., Barnett, T., Bouws, E., Carlson, H., Cartwright, D., Enke, K., Walden, H. (1973). Measurement of wind-wave growth and swell decay during the joint north sea wave project (JONSWAP). Hamburg: Duetches Hydrographisches Institut.

Hirji, K.F. (1997). A review and a synthesis of the fast Fourier transform algorithms for exact analysis of discrete data. Computational Statistics & Data Analysis. 25. 321–336.

Holland, K.T., Vinzon, S.B., Calliari, L.J. (2009). A field study of coastal dynamics on a muddy coast offshore of Cassino beach, Brazil. Continental Shelf Research. 29. 503–514.

Holmedal, L.E. & Myraug D. (2000). Combined tidal and wind driven flows and bedload transport over a flat bottom. Ocean Modelling.68. 37–56.

Holthuijsen, L. (2007). Waves in Oceanic and Coastal Waters. New York: Cambridge University Press.

Ijima, T. & Tang, F. (1966). Numerical calculation of wind waves in shallow water. 10th Conference of Coastal engineering (pp.38-45). Tokyo:ASCE.

Kinsman, B. (1965). Wind waves: their generation and propagation on the ocean surface. New Jersey: Prentice-Hall.

Kitaigorodskii S.A.(1962). Applications of the theory of similarity to the analysis of wind-generated wave motion as a stochastic process. Deep Sea Research and Oceanographic Abstracts (pp.105-117).

Luettich, R.A., Harleman, D.R.F., Somlydody, L. (1990). Dynamic behaviour of suspended sediment concentration in a shallow lake perturbed by episodic wind events. 35. 1050–1067

Maine, C. (2011). The flocculation dynamics of cohesive sediments in the St Lucia and Mfolozi estuaries, South Africa. South Africa: University of KwaZulu-Natal.

Mariotti, G. & Fagherazzi,S. (2012). Wind waves on a mudflat: the influence of fetch and depth on bed shear stresses. Continent Shelf Research.

Mehta, A.J. & Jiang, F. (1990). Some field observations on bottom mud motion due to waves. South Florida Water Management District. Florida

REFERENCES

Pierson, W. & Moskowitz, L. (1964). A proposed spectral form for fully developed wind seas based on the similarity theory of S.A. Kitaigorodskii. Journal of Geophysical Research, 5181-5190.

Ross, M.A. & Mehta, A.J. (1989). On the mechanics of lutoclines and fluid mud. Journal of Coastal Research. SI 5. 51–61.

Rügner, H., Schwientek, M., Egner, M., Grathwohl, P. (2014). Monitoring of event-based mobilization of hydrophobic pollutants in rivers: Calibration of turbidity as a proxy for particle facilitated transport in field and laboratory. Science of the Total Environment. 490. 191–198

Sherwood, C. & Wiberg, P. (2008). Calculating wave-generated bottom orbital velocities from suface-wave parameters. Computers & Geosciences, VOL, 1243–1262.

Sverdrup, H.U. & Munk, W.H. (1947). Wind, sea and swell: theory of relations for forecasting. U.S. Navy Hydrographic Office Publication. 601. 44.

Tananaev, N.I. & Debolskiy, M.V. (2014). Turbidity observations in sediment flux studies: Examples from Russian rivers in cold environments. Geomorphology. 218. 63–71.

Thijsse, J. (1948). Dimension of wind-generated waves. General Assembly of Association d'Oceanographie Physique (IGUU),80-81.

Tirok, K. & Scharler, U.M. (2014). Influence of variable water depth and turbidity in a shallow estuarine lake system - a modelling study. Estuarine, Coastal and Shelf Science. 146. 111–127.

Walmsley, J., Taylor, P., Salmon, J. (1989). Simple guidelines for estimating wind speed variations due to small-scale topographic features - an update. Climatological Bulletin, 1-16.

Weir, M., Hass, J. & Giordano, F. (2005). Thomas' Calculas: Eleventh Edition. Pearson Education.

Wiberg, P.L. & Sherwood, C.R. (2008). Calculating wave-generated bottom orbital velocities from surface-wave parameters. Computers & Geosciences. 34. 1243–1262

Young, I. & Verhagen, L. (1996). The growth of fetch-limited waves in water of finite depth. Part 1: The total energy and peak frequency. Coastal Enineering, 29, 57-48.

Young, I. (1997). The growth rate of finite depth wind-generated waves. Coastal Engineering, 32, 181-195.

Ziegler, A.C. (2002). Issues related to use of turbidity measurements as a surrogate for suspended sediment. Turbidity and other Sediment Surrogates Workshop. Reno

Chapter 3

Wind-driven waves in a shallow estuarine lake with muddy substrates: St Lucia, South Africa

3.1 Abstract

Wind-waves in shallow lakes or estuaries with muddy substrates can drive sediment re-suspension and cause high turbidities that can negatively impact the productivity of photosynthetic organisms. This investigation evaluates the efficacy of a simple semi-empirical model (Young & Verhagen, 1996) for predicting the wave characteristics in these systems in order to include their effects in ecosystem models. The southern basin of the St Lucia estuarine lake in South Africa was used for a case study. Average depths are about 1 m with fetches up to approximately 10 km. Substrate materials vary from sandy to muddy with deeper locations predominantly the latter. An array of pressure sensing wave poles was deployed to measure significant wave heights to compare with model predictions. The influence of the wind speed, fetch, fetch-averaged depth, and substrate composition were evaluated. Most of the observed waves were fetch limited during the conditions that prevailed during the two field trips. The results indicate that the model adequately captures the high energy wave events for persistent wind speeds and directions, but that there is considerable variability in its performance generally. Some of this variability can be attributed to difficulties in estimating appropriate fetch and depth parameters for variable winds and in the context of a lake with compound shape and variable bathymetry. There was no clear evidence of significant wave attenuation due to the muddy substrates.

3.2 Introduction

The biological functioning of shallow lakes or estuaries with muddy substrates can be significantly influenced by wind waves that drive sediment re-suspension and associated high turbidities. For example high turbidity affects primary production processes (Cloern, 1987) while zooplankton may also be adversely affected with reduced feeding rates and increased mortality rates (Carrasco *et al.*, 2013).

To apply simple quantitative biological models to explore these issues requires a means to estimate wave energy directly from easily accessible parameters such as wind speeds, fetches and depths. For shallow lakes and estuaries the growth of wind-waves is often affected by fetch and/or depth limited conditions. The prediction of wave characteristics under these conditions was addressed by Young & Verhagen (1996) who proposed a semi-empirical model based on an extensive field study conducted at Lake George in Australia. However, Young & Verhagen (1996) did not consider the effects of muddy substrates on the growth of wind-waves, since their case study site had sandy substrates. It is well known that waves can be attenuated by the dissipative effects of induced shear stresses within the fluid-mud layers of shallow systems (e.g. Elgar & Raubenheimer, 2008; Hsu *et al.*, 2013; Kranenburg *et al.*, 2011; Maa & Metha, 1990; Metha & Jiang, 1990; Sheremet & Stone, 2003; Winterwerp *et al.*, 2007, 2012). Apparently these effects have not yet been incorporated into simplified semi-empirical models.

Lake St Lucia is a large estuarine lake system located in KwaZulu-Natal, South Africa (Fig. 3.1). It is part of the iSimangaliso Wetland Park, which was declared a UNESCO World Heritage site in 1999. The area is also a Ramsar wetland of international importance due to its significant role as a biodiversity hotspot (Perissinotto *et al.*, 2013). The shallow lake conditions and muddy substrates make the estuarine habitat particularly susceptible to the effects of high turbidity due to the stirring effects of wind-driven waves. The system is increasingly threatened by increased catchment sediment yields due to land-use changes and land degradation. Similar challenges are faced by many estuarine and lake systems worldwide due to intensive developments within their catchments (e.g. Wolanski, 2007). There is a need to develop models that can be used to understand and evaluate the impacts of these changes, and to manage and mitigate them in the future.

This study aims to contribute towards developing and testing simplified models to investigate the above-mentioned issues. In particular a key question addressed was do substrate characteristics need to be explicitly included in the model?

3.3 Methods

3.3.1 Case study site

The St Lucia lake system comprises three interconnected basins – False Bay, North Lake and South Lake – that are linked to the sea via a 22 km long sinuous channel called the Narrows (Fig. 3.1(a)). The inlet to the system from the sea can close for

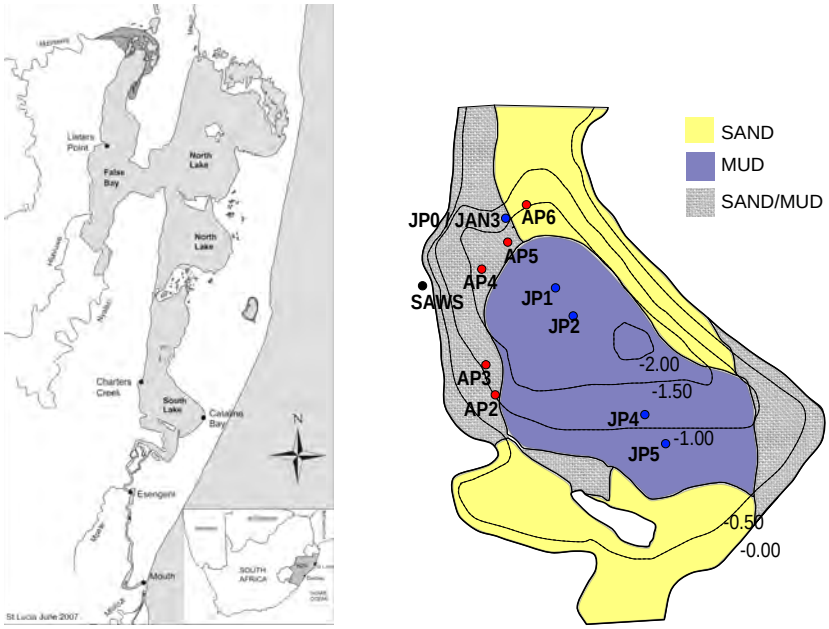

(a) (b)

Figure 3.1: (a) Map of St Lucia estuarine lake system on the east coast of South Africa (courtesy of N. Carrasco, 2013). (b) Detailed map of the southern basin showing bathymetry, substrate distribution, location of wave measuring stations (APx – stations used in April 2013, JPx – stations used in July 2013 and January 2014, for details see §4.3.2), and location of the weather station (SAWS).

prolonged time periods due to near-shore littoral transport processes (Lawrie & Stretch, 2011a,b). Tidal effects are present for about 14 km up the Narrows when the inlet is open - the lake itself is not tidal.

The lake has a surface area of approximately 350 km^2 and an average depth of 1.0 m when the inlet is open and when water levels are near the estuary mean water level (EMWL), which is a datum that is 0.25 m above sea level. When the inlet is closed the water level can differ strongly from EMWL depending on rainfall, river inflow and evaporation.

We measured waves in the lower part of Lake St Lucia South Lake in April, July 2013 and conducted a wind field investigation in January 2014(Fig. 3.1(b)). For the period of this investigation, the water level was ±0.3 m above EMWL. The lower South Lake has a surface area of approximately 30 km^2, extending approximately 6 km from north to south and 5 km east to west. The sediment of lower South Lake shows spatial variability with sandy areas around the edges and muddy area around the deeper center of the lake (Fig. 3.1(b)).

The wind climate is characterised by prevailing north-easterly and south-westerly winds, with north-east winds being dominant in the summer (Perissinotto *et al.*, 2013).

These wind directions were characteristic of the strongest winds observed during the course of this investigation. There is a strong diurnal cycle in the wind. Typical wind speeds during the day are $4\,\mathrm{m\,s^{-1}}$ or higher, whereas during the night wind speeds tend to be below $4\,\mathrm{m\,s^{-1}}$. Wind roses for the periods of our field trips are shown in Fig 3.2. The lighter night-time winds tend to come from the west and are thermally driven land breezes.

3.3.2 Field measurements

We measured waves at ten different locations over a total period of 15 days in April and July 2013 using pressure transducers (Fig. 3.1(b)). Each pressure transducer and its digital controller and logger was mounted inside a perforated tube to form a "wave pole" (Fig. 3.3). In April the wave poles were arranged approximately parallel to the main wind directions (north-easterly and south westerly) to provide data for wave growth along a varying fetch. The poles were placed at depths between 1 and 1.7 m with a mix of mud/sand sediments. The poles deployed in July were arranged in a way that kept the fetch fairly constant for the north-easterly wind direction and the depth at the poles ranged from 0.9 to 2.1 m with mainly muddy sediment. The water depth at each wave pole was measured using a survey staff. This served as a comparison to the average water depth measured by the pressure transducers.

In January 2014 an anemometer was mounted to a wave pole and deployed to validate the application of a wind speed correction factor. The anemometer was positioned approximately 1 m above the waterline and deployed at station JP0. This position was assumed to be far enough from the shoreline for the open water boundary layer to be fully developed.

Each pressure transducer was contained inside an air-tight, flexible plastic bag and attached to the end of an impermeable plastic manometer tube. The flexible plastic bag automatically adjusts for variations in atmospheric pressure so that the transducer measures differential pressures due to water level changes alone. The transducers were statically calibrated to establish the relationship between their voltage output and depth below the water surface. Measured pressures were logged to an SD memory card at a burst sampling frequency of 4Hz for durations of 5 minutes (1200 readings) every 15 minutes. The plastic manometer tube was weighted and the depth at which it was initially set was typically 0.5 m. The pressure transducer (MPX5010) had a range of 10 kPa (1 m of water) and an accuracy of about 0.5%. The output voltage of the sensor (0–5 V) was digitised with 10 bit resolution using an Arduino micro-controller. The electronics and battery power supply were packaged together with the pressure sensor in the waterproof bag installed at the top of the pole.

3.3.3 Data analysis

The recorded pressure data were transformed into significant wave heights (H_s) for each five minute sampling period. In this procedure, the pressure time series were decomposed into Fourier modes, each with a specific frequency. These modes were

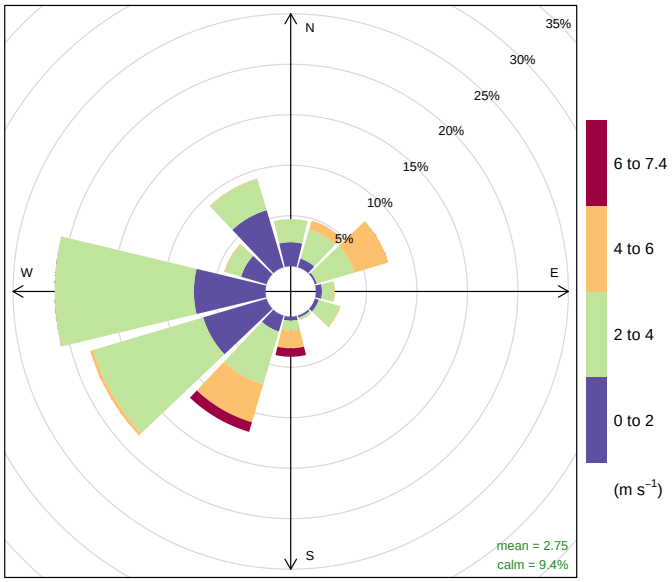

(a)

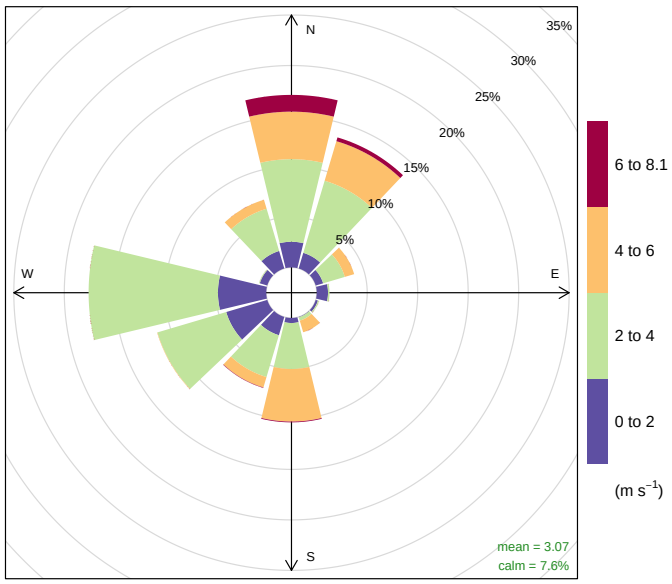

(b)

Figure 3.2: Wind roses for the two field trips in (a) April 2013, and (b) July 2013

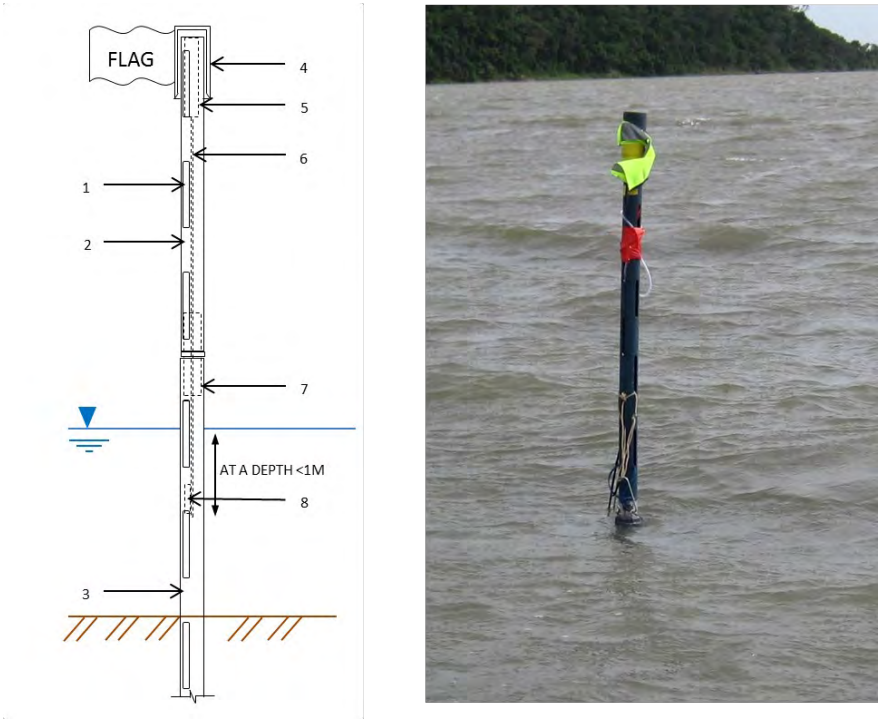

Figure 3.3: Schematic diagram of the wave pole components. the labelled items are: (1) plastic pole slots; (2) plastic pole; (3) metal base pole; (4) plastic cap; (5) differential pressure transducer device and data logger; (6) plastic manometer tube; (7) connection; (8) weight. A multiparameter sonde containing various sensors (temperature, salinity, pH, DO, turbidity) was attached to selected wave poles during their deployment.

individually corrected for attenuation of the pressure with depth according to linear wave theory. An inverse Fourier transform was then used to recreate the actual observed wave heights. The amplitude a of a surface wave of wavelength L and period T can be related to the pressure p measured at depth z in water of total depth h by (e.g. Holthuijsen, 2007)

$$\frac{p}{\rho g} = a\,\sin(kx - \omega t)\,\frac{\cosh\left(k\,(h+z)\right)}{\cosh(k\,h)} \tag{3.1}$$

with $k = 2\,\pi/L$, $\omega = 2\,\pi/T$, $L = (gT^2/2\pi)\tanh(k\,h)$, and where ρ is the water density and g is acceleration due to gravity. The significant wave height H_s can be computed as the average of the highest one third of the wave heights recorded during each five minute sampling period. Other parameters derived from the recorded pressure fluctuations

were the peak period and the average water depth.

Significant wave heights smaller than 50 mm were excluded from further analysis because the attenuation of the pressure signal from these small waves were not accurately resolved by the pressure transducer.

3.3.4 Wave Model

We used a simple semi-empirical model (Young & Verhagen, 1996, Y&V henceforth) to predict wave heights at the individual wave pole positions based on fetch, average depth over the fetch and wind speed. We then compared the predicted wave heights with the measured wave heights to test the efficacy of the Y&V model for Lake St Lucia. Our study site differs from the system used for calibration by Y&V by having a smaller surface area and having muddy sediment instead of sandy sediment. The fetch was estimated for each of the pole positions under the different wind directions using Google Earth^{TM} imagery. The average depth over the fetch was estimated using a bathymetry contour map given by (Hutchison, 1974, refer Fig. 3.1(b)).

Wind speeds and directions were provided by the South African Weather Service, which collects wind data from a weather station located near the western bank of the lake (SAWS in Fig. 3.1(b)) with the anemometer installed at a height of approximately 10 m .

The Y&V model is formulated in terms of non-dimensional quantities. The relevant dimensionless depth and fetch from the field measurements were calculated for each five minute data set at each wave pole position. These dimensionless values together with the corrected wind speeds were used as inputs to the model. The dimensionless forms of the wave energy (E), depth (d) and fetch (x) used for the model are defined by

$$\varepsilon = E\,\frac{g^2}{U_{10}^4}, \qquad \delta = d\,\frac{g}{U_{10}^2}, \qquad \chi = x\,\frac{g}{U_{10}^2}. \tag{3.2}$$

where U_{10} is a reference wind speed at a height of 10 m. Young & Verhagen (1996) suggested a semi-empirical relationship between ε, δ and χ given by

$$\varepsilon = C_0 \left[\tanh(C_1\ \delta^{0.75}) \tanh\left(\frac{C_2\ \chi^{0.57}}{\tanh(C_1\ \delta^{0.75})}\right)\right]^{1.74} \tag{3.3}$$

with constants $C_0 = 3.64 \times 10^{-3}$, $C_1 = 0.493$, and $C_2 = 3.13 \times 10^{-3}$. Equation 3.3 predicts the wave energy in the limits of both depth and fetch limited conditions and is consistent with results deduced from previous experimental data (Table 3.1).

Due to different characteristics of the boundary layer over land compared to water (Walmsley *et al.*, 1989) wind speeds should be corrected according to their direction and fetch over the water at individual wave pole locations. Winds measured at the weather station were corrected as described by Young & Verhagen (1996), whence

$$U_x = U_i + \Delta R\ U_i \tag{3.4}$$

where U_i is the (measured) reference wind speed prior to crossing the shoreline, U_x is the wind speed at a fetch x downwind from the shoreline crossing point, and ΔR is a correction factor given by

$$\Delta R = 0 \qquad \text{for } z \geq \delta_i \tag{3.5}$$

$$\Delta R = \frac{\left(\ln(z/z_0)\ \ln(z/z_0')\right)}{\left(\ln(z/z_0')\ \ln(\delta_i/z_0)\right)} - 1 \qquad \text{for } z < \delta_i \tag{3.6}$$

where z is the height of the reference wind, z_0 is the roughness length over water, z_0' is the upwind terrestrial roughness length, and δ_i is the internal boundary layer height over water given by

$$\delta_i = 0.75\, z_0 \left(\frac{x}{z_0}\right)^{4/5}. \tag{3.7}$$

The roughness length over the water z_0 is assumed to vary with wind speed (Young & Verhagen, 1996) as

$$z_0 = A\ \frac{u_*^2}{g} \tag{3.8}$$

$$u_*^2 = C_{10}\, U_{10}^2 \tag{3.9}$$

$$C_{10} = (0.8 + 0.065\, U_{10}) \times 10^{-3} \tag{3.10}$$

where A=0.0185, u_* is the friction velocity, U_{10} is the wind speed at a reference height of 10 m, and C_{10} is a drag coefficient.

After experimenting with various terrestrial roughness lengths appropriate for the case study site (≈ 0.5 m) it was evident that the wind correction factor was generally close to unity i.e. $\Delta R \approx 1$. For simplicity this value was subsequently adopted as a uniform wind correction for all locations and wind directions.

Once the measured wind-speeds have been corrected for roughness changes, and given the measured fetch and depth parameters at each wave pole and for each wind direction, the significant wave height may be predicted from Eqn. 3.3 using the definition $H_s = 4\sqrt{E}$. These predicted wave heights can then be compared with the measured wave heights from the wave poles.

Table 3.1: Asymptotic limits of Eqn. 3.3 (Young & Verhagen, 1996).

Limiting Conditions	**Equation 3.3**
Depth limited: $\chi \to \infty$	$\varepsilon = 1.06 \times 10^{-3}\ \delta^{1.3}$
Fetch limted: $\delta \to \infty$	$\varepsilon = 1.6 \times 10^{-7}\ \chi$
$\chi \to \infty$, $\delta \to \infty$	$\varepsilon = 3.64 \times 10^{-3}$

For the pole-anemometer configuration set up in January the measured wind speed was expected to be be higher than the wind speed recorded at the South African

Weather Station. No wind correction was applied when developing the model wave heights in this case as wind data was measured insitu. The suitability of the correction factor could therefore only be inferred based on the performance of the Young & Verhagen equation using the insitu wind measurement.

3.4 Results

3.4.1 Measured wind and wave time series

The range of depths, fetches, and wave heights sampled during the field experiments at each of the wave pole locations (Fig. 3.1(b)) are summarised in Table 3.2. Maximum fetches were about 10 km and mostly associated with winds from northerly directions. Fetch-averaged depths during the July field trip were generally larger than for the April field trip due to the re-positioning of the wave poles.

Table 3.2: Range of depths at sampling positions, average depths, significant wave heights and fetches observed during field trips. The average depth is the depth at each sampling position averaged over the fetch (which varies with the wind direction).

Sampling Locations (refer Fig. 3.1(b))	Pole Depth (mm)		Fetch Avg Depth (mm)		Fetch (m)		H_s (mm)	
	min	max	min	max	min	max	min	max
April field trip								
AP2	1540	1850	760	1680	660	11600	10	310
AP3	1420	1730	810	1650	50	11000	10	350
AP4	1090	1380	930	1630	600	9600	10	330
AP5	890	1170	930	1630	1000	9000	10	310
AP6	710	990	890	1600	1200	9300	10	270
July field trip								
JP0	820	1070	540	1330	700	10200	10	240
JP1	1640	2160	890	1390	650	10300	10	370
JP2	1420	2330	950	1590	1400	9700	10	380
JP4	1970	2310	570	1440	1700	7500	10	410
JP5	1920	2180	350	1370	1800	10300	10	350

Figure 3.4 shows time histories of water levels, wave heights and wind vectors measured during the two field trips in April and July 2013. There are strong diurnal variations in the wind speed at this location, which are evident in the time series. During the night-time hours wind speeds typically reduce to 4 ms^{-1} or less, and comprise mainly land breezes from the west. Winds greater than 4 ms^{-1} generally occur during the day (peaking in the afternoons) and are typically from the south-west or north-east (Fig. 3.2). It is these stronger winds that drive the generation of waves in the lake with significant waves heights typically in the range 200 – 400 mm.

It is evident from Fig. 3.4 that waves increase rapidly as the wind increases and also dissipate rapidly once wind speeds reduce again. The increases in wave energy are accompanied by re-suspension of fine muddy sediments that make the water column highly turbid.

In addition to the generation of waves the surface wind stress also drives significant water exchanges between the lake basins that are evident as changes in average water levels in Fig. 3.4. When the wind blows from southerly directions water is pushed north in the system and water levels fall in the South Lake, and vice versa for winds from northerly directions. These wind setup processes and their time scales have been described in detail by Hutchison & Midgely (1978); Schoen *et al.* (2014). Water level changes of up to 400 mm were observed during the field study (Fig 3.4). During calm periods after high winds the system relaxes towards a state where the water levels across all the basins are equal.

During the April field trip most of the energetic wave events were driven by winds from the south-south westerly direction (Fig. 3.2). The pole arrangement used (Fig. 3.1(b)) means that almost half of the data set experienced similar fetch conditions. During the July field trip the strongest winds were more evenly split between the northerly and the southerly directions. Fetches for the southerly winds were generally slightly larger than those for northerly winds for this pole arrangement.

3.4.2 Comparisons with Young & Verhagen model

Scatter plots show general consistency between the measured and modelled wave heights (Figure 3.5). The model shows some bias towards under prediction of wave heights for small fetches and/or small depths, but its performance improves at intermediate fetch and depth values. However, considerable scatter is evident in the data.

A more detailed comparison between the model and measurements is given in Figures 3.6, 3.7 & 3.8 that show a series of non-dimensional plots of measured wave energy ε as a function of fetch number χ. Values for the non-dimensional depths δ are colour-coded to the data points.

Wave energies predicted by the Young & Verhagen (1996) model for various depth numbers are plotted for comparison with the measurements, and indicate which conditions were fetch or depth limited in terms of wave growth.

It is evident that most of the measurements were in fetch-limited or transitional conditions according to the model, although there are also significant occasions that experienced depth-limited wave growth. The trends in the measurements are broadly consistent with the model but again show considerable variability as is evident in the scatter of the data. Figure 3.7(a) & (b) only show data with depth numbers $\delta < 0.2$ to illustrate depth limiting effects on the wave growth. Note that according to the model all the measured data should lie below the $\delta = 0.2$ line in these plots. Similarly, in Fig. 3.8(a) & (b) only data with depth numbers $\delta > 0.2$ are shown, which according to the model should all lie above the $\delta = 0.2$ line in the plots. There are a significant number of measurements that lie outside the predicted bounds i.e. the measured wave energies are lower than predicted by the model. Given the scatter in the data it is not

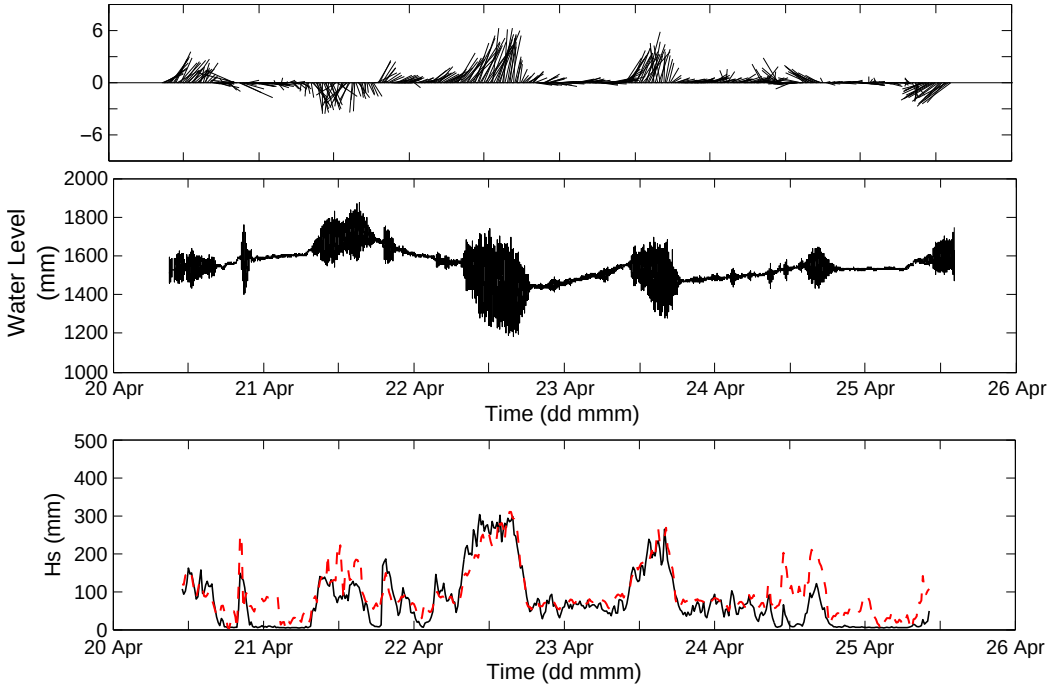

(a)

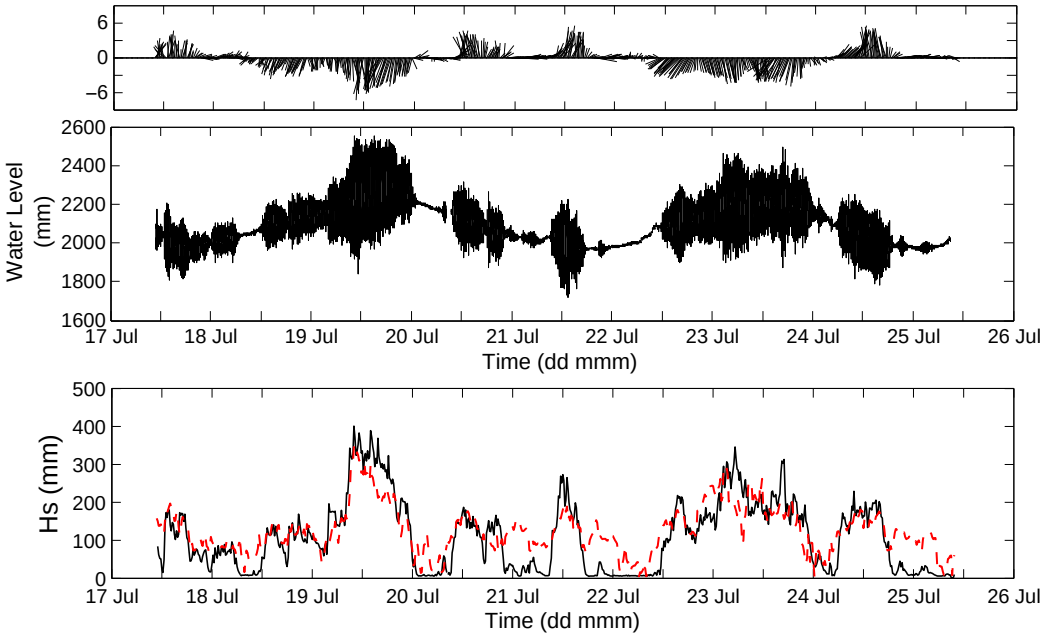

(b)

Figure 3.4: Wind vector (top panel), water level (middle panel) and measured and predicted significant wave height time series for (a) April field trip, pole AP3; (b) July field trip, poles JP4 and JP5 (concatenated). The pole positions are shown in Fig 3.1(b). Wind measurements (uncorrected) are from the weather station shown as location SAWS in Fig 3.1(b). For the H_s time series the solid black lines (—) are measured data and the dashed red lines (- - -) are model predictions.

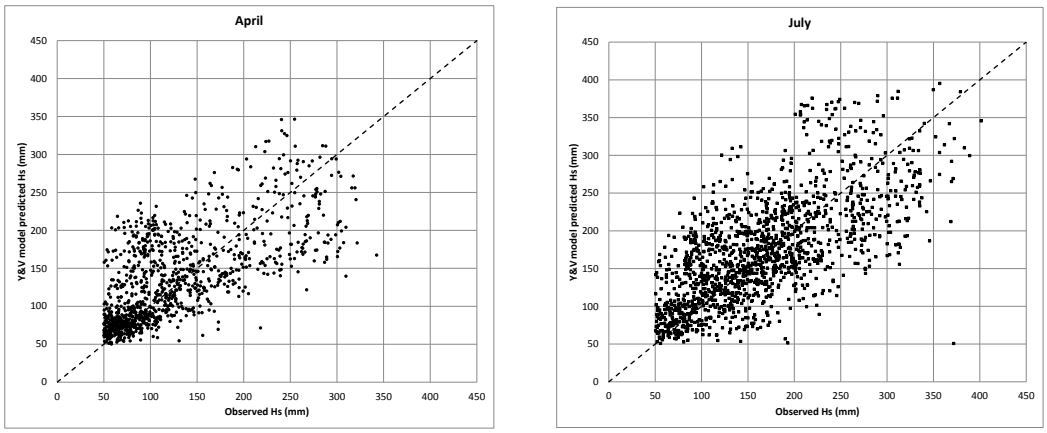

(a) (b)

Figure 3.5: Scatter plots of predicted versus observed H_s for: (a) April field data; (b) July field data.

possible to unambiguously attribute these effects to wave attenuation associated with muddy substrates, but that is one possible explanation.

Fig 3.7(a) & (b) reveals that the model tends to consistently overestimate the wave energy for small fetch numbers $\chi < 100$ and depth numbers $\delta < 0.1$. These data are from the April field trip and come from wave poles near the western side of the basin (AP2, AP3), and for wind from the south/south-west.

Samples of measured and modelled wave height time series indicate that the major wind-wave events are generally well captured by the model when the wind comes from specific directions (Fig 3.4). When the wind speed and/or direction changes the model can produce large prediction errors, which seems to be associated with estimation of the appropriate fetch and depth parameters that are applicable during those periods.

In Figure 3.9 the Y&V equation has been applied using in-situ wind speeds measurements and no wind correction factor. The modelled wave heights match the trends of the observed significant wave heights with RMSE error remaining below 20mm in most cases.

Error statistics for the model predictions are summarised in Table 3.3. There is some bias evident from the non-zero mean errors while about two thirds of the H_s measurements are predicted to within about 20 % of the maximum values given in Table 3.2.

3.5 Discussion and Conclusions

In this study we have tested the application of the Young & Verhagen (1996) semi-empirical model for predicting wave heights in a shallow estuarine lake with compound shape and variable bathymetry. A notable difference from previous applications of the

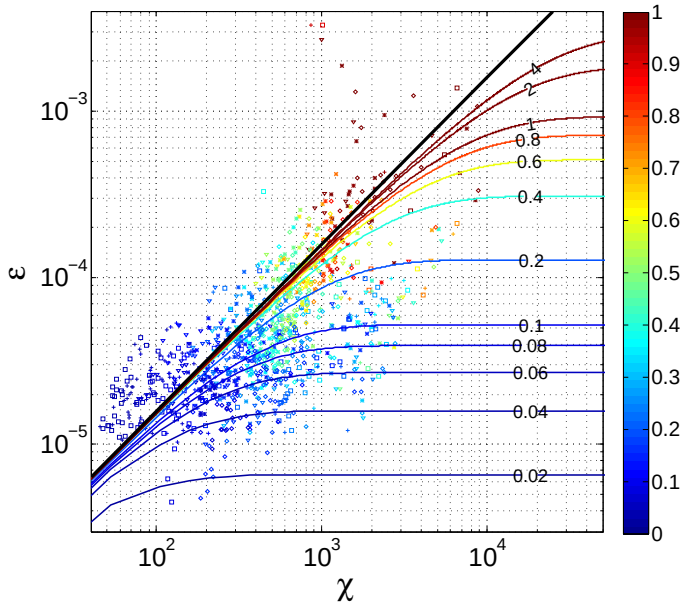

(a)

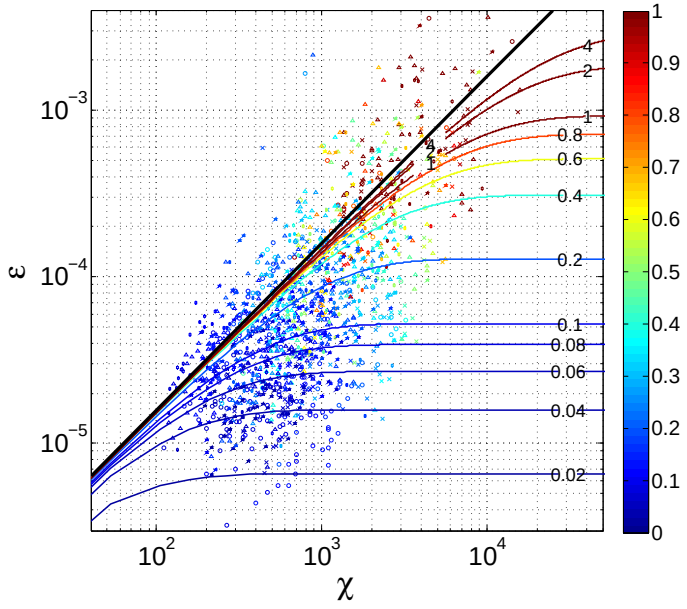

(b)

Figure 3.6: Non-dimensional plots of observed wave energy (ε) versus fetch (χ) for various depths (δ, shown colour-coded). Wave energies predicted by the Young & Verhagen (1996) model are shown as coloured lines for comparison with the measurements. (a) April: all data, (b) July: all data.

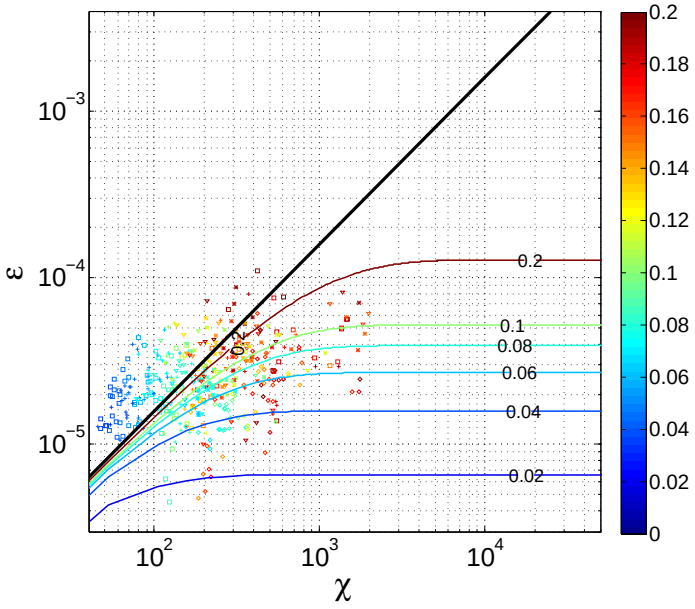

(a)

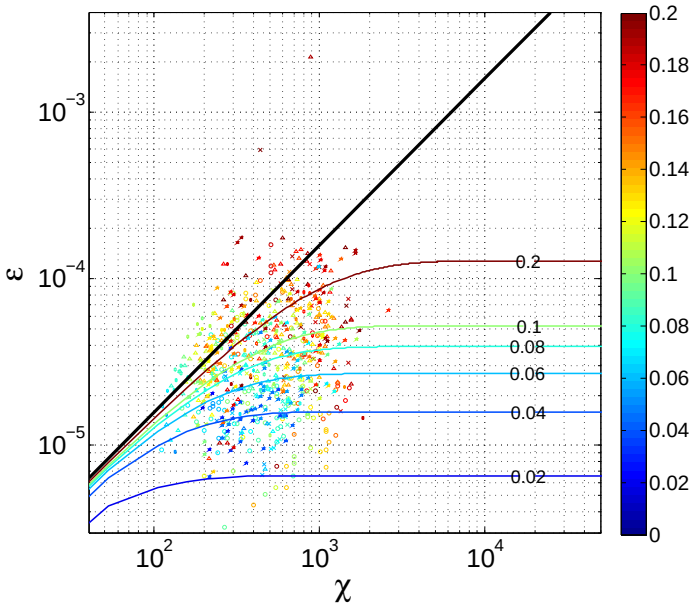

(b)

Figure 3.7: Non-dimensional plots of observed wave energy (ε) versus fetch (χ) for various depths (δ, shown colour-coded). Wave energies predicted by the Young & Verhagen (1996) model are shown as coloured lines for comparison with the measurements. (a) April: $\delta < 0.2$, (b) July: $\delta < 0.2$.

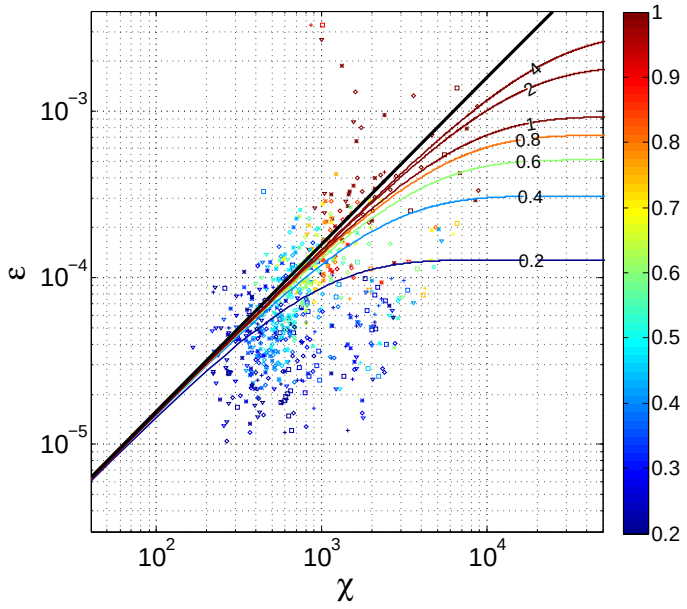

(a)

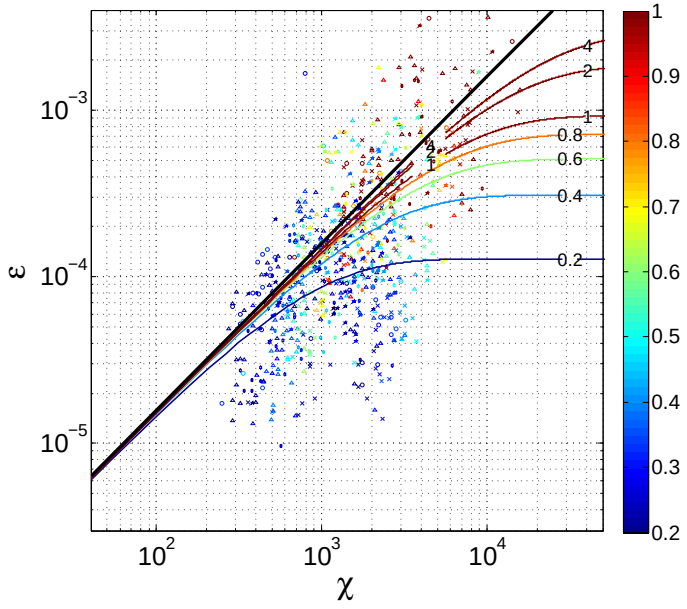

(b)

Figure 3.8: Non-dimensional plots of observed wave energy (ε) versus fetch (χ) for various depths (δ, shown colour-coded). Wave energies predicted by the Young & Verhagen (1996) model are shown as coloured lines for comparison with the measurements. (a) April: $\delta > 0.2$, (b) July: $\delta > 0.2$.

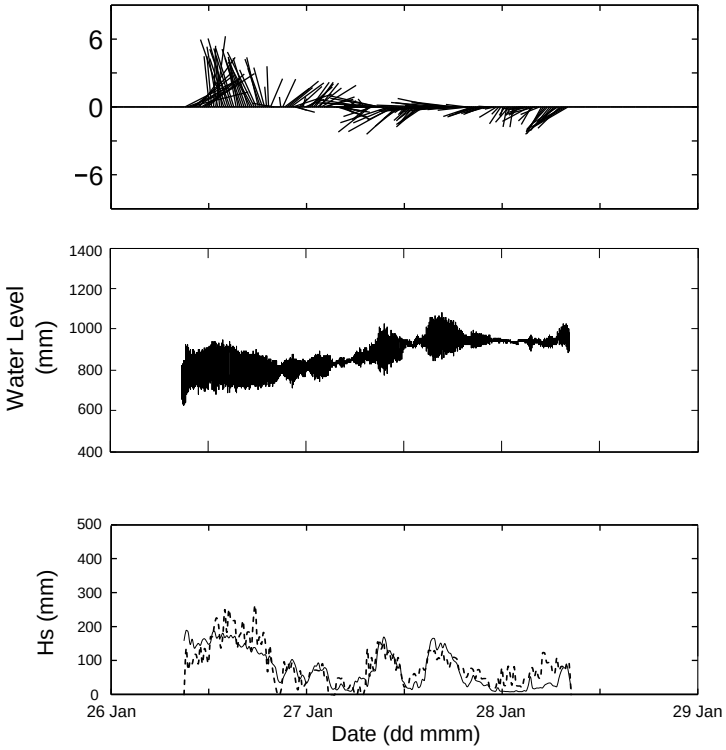

Figure 3.9: The top panel depicts a wind vector plot of the winds measured in January using a wave pole mounted with an anemometer. The anemometer was positioned at a height of ± 1 m above still water level. The middle panel depicts the depth of the water surface as measured using a pressure transducer. The bottom panel depicts the measured significant wave heights (solid line) and the Y&V equation predicted significant wave heights (dashed line) for the same time period. Note that in this case no wind correction factor was applied.

model is the substrate's composition at our case study site. St Lucia comprises large areas with soft, unconsolidated muddy substrates, particular in the deeper locations, while previous case studies have focussed mainly on systems with sandy substrates. This difference was a key motivation for the present study, namely to evaluate how muddy substrates affect wind-wave predictions from simple models.

The comparison between modelled and measured significant wave heights shows broad consistency but with considerable variability in the results. There are examples of both significant underestimation as well as overestimation of wave energy, but the reason(s) for these errors are difficult to isolate. Some of the model's underestimation seems to be associated with short fetch and/or shallow water, which is consistent with previously reported results (e.g. Young, 1997).

Clear evidence of wave attenuation due to the influence of muddy substrates was not

Table 3.3: Error statistics for each wave pole sampling location. Errors are defined as the difference between predicted and measured wave heights. The statistics are the root mean square of the errors (rmse), standard deviation of the errors (sdev), and the mean errors (mean).

Measurement Locations (refer Fig. 3.1)	H_s Error Statistics (mm)		
	rmse	sdev	mean
April field trip			
AP2	65	65	7
AP3	60	59	-6
AP4	56	56	3
AP5	39	38	7
AP6	37	35	-11
July field trip			
JP0	68	62	29
JP1	71	62	35
JP2	58	54	7
JP4	43	42	-10
JP5	50	49	-11

identified from the data. These effects, if present, may have been masked by scatter in the results. The compound shape of the lake system means that the estimation of the applicable fetch and depth parameters is difficult and prone to error, which may explain much of the variability in the data and model predictions. For example small changes in wind direction can make large differences in the estimated fetch and associated fetch-averaged depths. Furthermore the method of correcting the wind from a single terrestrial weather station to account for roughness changes over the water is also difficult to do accurately and can significantly impact model predictions.

If simple semi-empirical models such as the Young & Verhagen model are to be used to model wind-wave generation in shallow, muddy systems with complex geometry, our results suggest that considerable care is required to accurately specify insitu wave-generation parameters such as wind speed, direction, fetch, and fetch-averaged water depth. The simultaneous measurement of insitu wind speeds and directions for calibration of the wave-generation model may reduce some of these uncertainties. However, alternative modelling approaches, such as the 2D spectral wave model SWAN (Booij *et al.*, 1999; Kranenburg *et al.*, 2011; Winterwerp *et al.*, 2007), can account for complex lake geometry and bathymetry in a natural way and may therefore be preferable in these cases.

Acknowledgments

The iSimangaliso Wetland Park Authority for supporting this research. The SA National Research Foundation and SANPAD for funding. Julia Schoen for extensive help with field work

and data analysis. Zane Thackeray for the wave data-loggers. Caroline Fox for field support. Henk-Jan Verhagen for his wave analysis Matlab code. Sydney Mpungose and Logan Govender for fabricating field equipment.

References

Booij, N., Ris, R. C., and Holthuijsen, L. H. (1999). A third-generation wave model for coastal regions. Part I: Model description and valida- tion. J. Geophys. Res., 104(C4), 7649 – 7666.

Carrasco, N., Perissinotto, R., Jones, S. (2013). Turbidity effects on feeding and mortality of the copepod Acartiella natalensis (Connell and Grindley, 1974) in the St. Lucia Estuary, South Africa. Journal of Experimental Marine Biology and Ecology, 45–51.

Cloern, J. (1987). Turbidity as a control on phytoplankton biomass and productivity in estuaries. Continental Shelf Research, 7, 1367–1381.

Elgar, S., & Raubenheimer, B. (2008). Wave dissipation by muddy seafloors, Geophys. Res. Lett., 35, L07611, doi:10.1029/2008GL033245.

Holthuijsen, L. (2007). Waves in Oceaninc and Coastal Waters. New York: Cambridge University Press.

Hsu, W. Y., Hwung, H. H., Hsu, T. J. Torres-Freyermuth, A. and Yang, R. Y. (2013). An experimental and numerical investigation on wave-mud interactions. J. Geophysical Research: Oceans, 118, 1–16, doi:10.1002/jgrc.20103.

Hutchison, IPG., (1974). St Lucia Lake and estuary - hydrographic data. Report No. 3/74, Hydrological Research Unit, University of the Witwatersrand, Johannesburg, South Africa.

Hutchison, IPG & Midgely, DC., (1978). Modelling the water and salt balance in a shallow lake. Ecological Modelling, 4, 211–235.

Kranenburg, W. M., Winterwerp, J. C., de Boer, G. J., Cornelisse, J. M. & Zijlema, M. (2011). SWAN-Mud: Engineering Model for Mud-Induced Wave Damping. J. Hydraul. Eng., 2011,137, 959 – 975.

Lawrie, R.A. & Stretch, D.D., (2011a). Anthropogenic impacts on the water and salinity budgets of St Lucia estuarine lake in South Africa. Estuarine, Coastal and Shelf Science, 93, 58 – 67.

Lawrie, R.A. & Stretch, D.D., (2011b). Occurrence and persistence of water level/salinity states and the ecological impacts for St Lucia estuarine lake, South Africa. Estuarine, Coastal and Shelf Science, 95, 67–76.

Maa, J. P. Y. & A. J. Mehta (1990). Soft mud response to water-waves, J. Waterways, Port, Coastal, Ocean Eng., 116(5), 634–650.

Mehta, A., & Jiang, F. (1990). Some field observations on bottom mud motion due to waves. Florida: South Florida Water Management District.

Perissinotto R., Stretch, D.D., Taylor, R.H. (eds), (2013). *Ecology and Conservation of Estuarine Ecosystems: Lake St. Lucia as a Global Model*. Cambridge University Press.

Schoen, J, Stretch, DD & Tirok, K., (2014). Wind-driven circulation in a shallow estuarine lake: St Lucia, South Africa. *Estuarine, Coastal and Shelf Science*, submitted.

Sheremet, A., & Stone, G. W. (2003). Observations of nearshore wave dissipation over muddy sea beds, J. Geophys. Res., 108(C11), 3357, doi:10.1029/2003JC001885.

Walmsley, J., Taylor, P., & Salmon, J. (1989). Simple guidelines for estimating wind speed variations due to small-scale topographic features - and update. Climatological Bulletin.

Winterwerp, J. C., de Graaff, R., Groeneweg, J. and Luijendijk, A. (2007). Modelling of wave damping at Guyana mud coast. Coastal Engineering., 54(3), 249 – 261.

Winterwerp, J. C., de Boer, G. J., Greeuw, G. and van Maren, D.S. (2012). Mud-induced wave damping and wave-induced liquefaction. Coastal Engineering., 64, 102 – 112.

Wolanski, E., (2007). *Estuarine Ecohydrology*. Elsevier.

Young, I.R. (1997). The growth rate of finite depth wind-generated waves. Coastal Eng., 32(2-3), 181–195.

Young, I.R. & Verhagen, L. (1996). The growth of fetch limited waves in water of finite depth. Part 1. Total energy and peak frequency. Coastal Engineering, 29, 47–78.

Chapter 4

Sediment re-suspension in a shallow estuarine lake with muddy substrates: St Lucia, South Africa

4.1 Abstract

Wind-driven sediment re-suspension affects the physical and biological environment of the water column in shallow estuarine lakes. This study investigated the relationship between wind-driven waves and suspended sediment concentration (SSC) using the South Lake of Lake St Lucia, South Africa as a case study. A series of wave poles were deployed over a period of twenty days. The wave poles measured significant wave height and turbidity. Sampling locations had different substrate sediment compositions and depths. The resulting turbidity dynamics were used to calibrate a depth averaged model of suspended sediment concentration. The calibrated model performed best in the muddy regions of the lake and was able to simulate the re-suspension dynamics more accurately than the settling dynamics. Peak suspended sediment concentration levels were best captured for the site located in the deeper muddy region. This model provides a means for spatially explicit prediction of suspended sediment concentrations. Models such as this can be used to understand the forcing mechanisms for primary producer growth and distribution or to improve sediment budget calculations.

4.2 Introduction

The suspended sediment concentration (hereinafter SSC) has a marked effect on the water column's physical and chemical properties, ecology and benthic geomorphology (Cloern, 1987; Liu *et al.*, 2014; Wu & Hua, 2014). Wind driven waves control sediment re-suspension and associated high turbidities in shallow lakes and estuaries.A shallow

lake habitat's water quality is directly affected by SSC. Wu & Hua (2014) describes how SSC influences endogenous phosphorous release a common indicator for eutrophication levels.

Light attenuation caused by high turbidities affects phytoplankton and macrophyte species' distribution and abundance especially within the limnetic zone where palagic algae are found(Bailey & Hamilton, 1997; Tirok & Scharler, 2014). Primary producers' reproductive abilities are sensitive to high turbidities (Cloern, 1987) while zooplankton may experience reduced feeding and increased mortality rate (Carrasco *et al.*, 2013). Sedimentary infilling of silt and clays from the surrounding area, fluvial sources and slow-moving currents cause shallow lakes and estuaries to often be characterized by a muddy benthic substrate.(Castaing & Allen, 1981).

Sediment re-suspension is a function of wave and current induced shear stresses near the lake bottom (Bailey & Hamilton, 1997; Brand *et al.*, 2010; Wiberg & Sherwood, 2008). Bed shear stresses are directly related to wind-driven wave amplitudes and periods. The orbital velocity of waves with a longer period and wavelength are able to extend their effect to greater depths than their shorter counterparts (Wiberg & Sherwood, 2008).

Directly modelling suspended sediment dynamics enables us to anticipate and understand the reaction of the biological and physical environment within shallow lakes. Existing research has modelled suspended sediment dynamics in lakes such as Lake Balaton (Luettich *et al.*, 1990), Lake Okeechobee (Jin & Ji, 2001) and Taihu Lake (Wu *et al.*, 2013) which are 20 to 75 times larger in surface area compared to our study site. Studies were also conducted in Esteros del Ibera (Cozar *et al.*, 2005) which is of a similar size to Lake St Lucia's South Lake.

These models can assist in the study of primary producer dynamics, sediment load management and sediment distribution models as well as and assisting with water quality monitoring for Lake St Lucia. The Luettich *et al.* (1990) model is one example of a sediment re-suspension model which may be applied in shallow lakes. The depth-averaged re-suspension model considers wave activity in relation to bed characteristics, sediment settling velocity and depth to determine SSC in low advective current conditions.

The research questions for this paper are as follows: can a simple depth averaged model successfully predict the re-suspension dynamics and SSC in Lake St. Lucia's South Lake? And do the model's parameters have to be adapted for varying benthic composition?

4.3 Methods

4.3.1 Case study site

Lake St Lucia is located in northern KwaZulu-natal on the eastern coast of South Africa at coordinates $28^o00'25.96''S$, $32^o28'50.58''E$. The lake comprises three interconnected basins - False Bay, North Lake and South Lake - that are linked to the sea via a

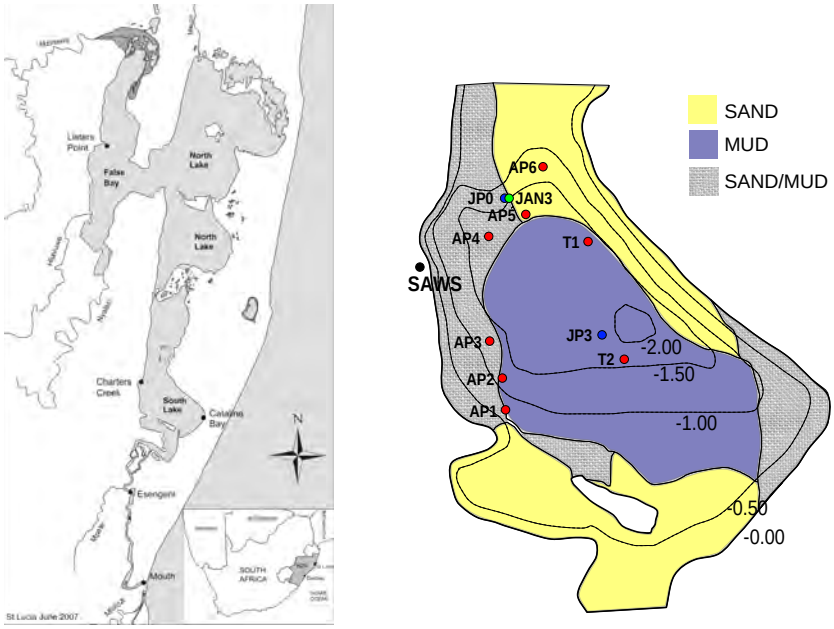

(a) (b)

Figure 4.1: (a) Map of St Lucia estuarine lake system on the east coast of South Africa (courtesy of N. Carrasco, 2013). (b) Detailed map of the southern basin showing bathymetry, substrate distribution, location of wave measuring stations (APx – stations used in April 2013, JPx – stations used in July 2013, and JAN3 – the station used in January 2014. For details see 4.3.2), and location of the weather station (SAWS).

22 km long sinuous channel called the Narrows (Figure 4.1(a)). The inlet to the system from the sea can close for prolonged time periods due to near-shore littoral transport processes (Lawrie & Stretch, 2011a,b; Perissinotto *et al.*, 2013). Tidal effects are present for about 14 km up the Narrows when the inlet is open - the lake itself is not tidal.

The lake has a surface area of approximately 328 km^2 and an average depth of 1.0 m when the inlet is open and when water levels are near the estuary mean water level (EMWL), a local datum that is 0.25 m above sea level (Lawrie & Stretch, 2011a). When the inlet is closed the water level can differ strongly from EMWL depending on rainfall, river inflow and evaporation. Field work was carried out in the southern half of South Lake (Figure 4.1) between April 2013 and January 2014. The average water level was ±0.3 m above EMWL during this period. The southern basin of South Lake has a surface area of approximately 30 km^2, extending approximately 6 km from north to south and 5 km east to west. The bed sediments vary spatially and generally comprise more sand around the edges with finer sediments in the deeper areas (Figure 4.1(b)). Cyrus (1988) describes how the lake water in South Lake is known to be clear in the east and turbid to the west which suggests a spatial difference in re-suspension dynamics.

The wind climate at St Lucia is characterised by prevailing north-easterly and south-westerly winds that drive significant inter basin water exchanges between North and South Lake. There is a strong diurnal cycle in the wind. Wind speeds during the day are typically 4 m.s^{-1} or higher, whereas during the night they tend to be below 4 m.s^{-1} (Schoen *et al.*, 2014).

4.3.2 Field measurements

Waves and turbidity were measured at several different locations (Figure 4.1(b)) over a total duration of 20 days between April 2013 and January 2014.

Wave characteristics were measured using a series of pressure transducers positioned throughout South Lake (see Zikhali *et al.* (2014)). Wave-induced pressures were logged to an SD memory card at a burst sampling frequency of 4 Hz for durations of 5 minutes (1200 readings) every 15 minutes. The pressure transducer and its digital micro-controller were mounted in an airtight bag contained by a perforated tube to form a 'wave pole' (Figure 4.2). Measurement locations were selected to provide variability in terms of benthic sediment composition. The three types of sediment compositions identified were sand, mud and sand/mud mixtures as described by Fortuin (1992) (see also Perissinotto *et al.*, 2013, Fig 9.5).

The Folk (1954) classification system defines mud (silts and clay) as particles smaller than 63 μm in diameter and sand to be $\geq$ 63 to 2000 μm in diameter (a similar grain size classification is noted by Das (2010)). This classification system was used in the study by Fortuin (1992) to develop the sediment distribution map shown in Figure 4.1. Sediment core samples were collected at each pole station for analysis using a Malvern Mastersizer 2000 that uses laser diffraction to measure grain size distributions for particles up to 2000 μm.

Turbidity was measured using YSI multi-parameter water quality sondes (models 6920 V2 and EXO2). A YSI sonde was attached to the side of each wave pole during deployment. Two sondes were deployed during the same time period for the July and the January field trips to investigate correspondence between results. Sondes were submerged to a depth that ensured submergence even in high wave conditions, but were kept near enough to the surface to allow for daily inspection. Each sonde was configured to sample and record turbidity at 15 minute intervals. Turbidity was measured in Nephelometric Turbidity Units (NTU) and a calibration was done to convert NTU data to SSC. Turbidity measurements based on optical backscatter can depend on the composition and size distribution of the re-suspended material in the water column. This introduces calibration errors where the suspended particle size distribution varies. Suspended sediment solutions were passed through filter membranes which were then dried and weighed to ascertain the amount of SSC required to produce a given level of turbidity. The sediment sample used for calibration was drawn from the muddy central region of the lake during the January field trip. Vertical turbidity profiles were also compiled from various points throughout the lake to ascertain whether a turbidity gradient was evident and whether the assumption of uniform mixing was valid.

In April the wave pole was positioned in a region of predominantly sand/mud with

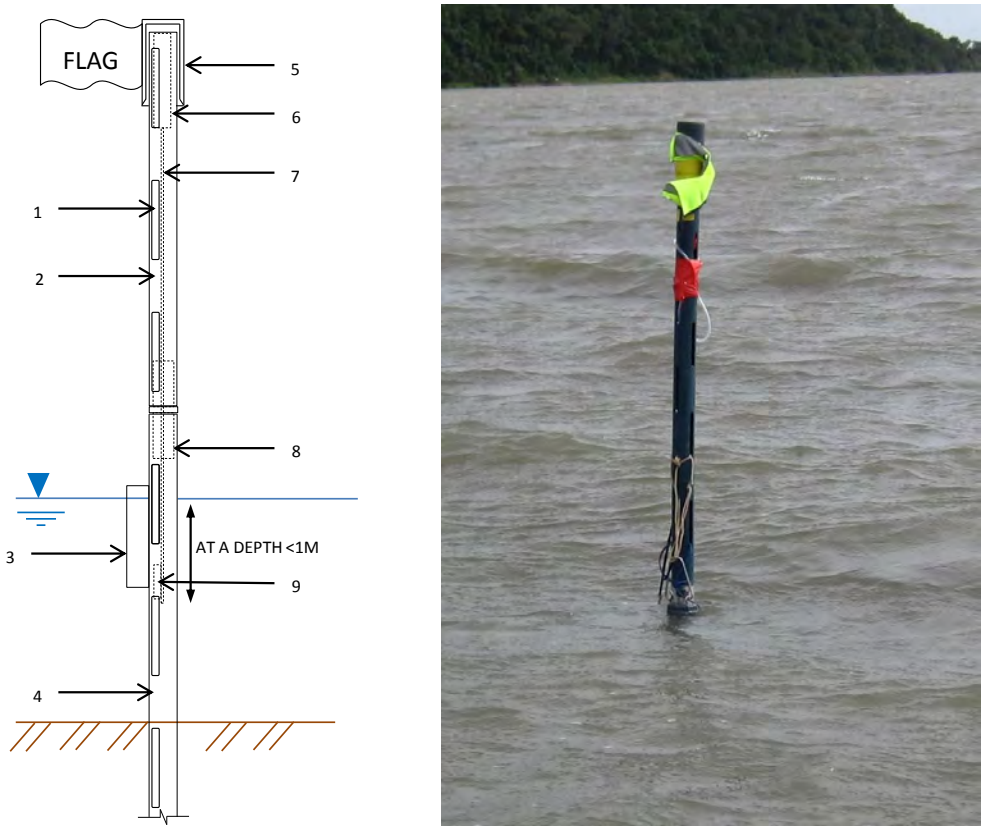

Figure 4.2: Schematic diagram of the wave pole components. the labelled items are: (1) plastic pole slots; (2) plastic pole; (3) YSI multiparameter sonde; (4) metal base pole; (5) plastic cap; (6) differential pressure transducer device and data logger; (7) plastic manometer tube; (8) connection; (9) weight.

an average depth of 1.5 m. Two poles were deployed in July, one in the sandy region to the North of South lake and the second nearer to the deeper, muddier middle. The average depth at the poles deployed ranged from 0.9 m at the sandy region to 2.1 m at the muddy region. The pole deployed in January was positioned in the same sandy region as the pole deployed in July with an average depth at the pole of 0.9 m. This afforded the opportunity to perform a comparison of the re-suspension conditions in that region for two separate times.

The water depth at each wave pole was measured using a survey staff. This allowed us to gauge the accuracy of average water depth changes derived from the pressure transducers' measurements. The average depth of the lake was measured near the weather station by way of a survey staff attached to the jetty.

4.3.3 Data analysis

Recorded pressure data was used to derive significant wave heights (H_s) for each five minute sampling period. These significant wave heights were then used in a deterministic model to establish the wave-induced model SSC for comparison with the observed SSC (Luettich *et al.*, 1990). The model parameters were optimised by reducing the mean squared error between the modelled and observed data using the Solver optimisation tool in Microsoft Excel. Error analyses were performed to determine under which conditions the model performed best using an agreement index and an efficiency index. The agreement index is a measure of agreement between the model and the observed values with a peak agreement value of 1.0. The co-efficient of efficiency ranges from negative infinity to 1.0, with higher values indicating a better model and negative values indicating that the observed mean is a better predictor than the model (Legates & McCabe, 1999).

4.3.4 Suspended sediment concentrations model (SSC)

The model developed by Luettich *et al.* (1990) describes suspended sediment dynamics in wave-influenced shallow lakes that are well mixed and where lateral advection is negligible. The model was developed and tested in the 600 km^2 Lake Balaton (Hungary) with an average depth of 3.2 m, and a bed comprising silt and clays.

Following Luettich *et al.* (1990) a simplified model for depth-averaged SSC based on a local sediment mass balance can be expressed as

$$\frac{dc}{dt} = -\frac{w_s}{h}(c - c_e) \tag{4.1}$$

where c is a depth averaged sediment concentration, w_s is a representative sediment settling velocity (assuming uniform vertical distribution of sediment throughout the water column), and c_e represents an equilibrium concentration where re-suspension and settling processes are balanced in a steady state situation.

Assuming a constant wave period and no change in depth for Δt, the concentration c_e is related to wave-driven re-suspension by

$$c_e(t) = c_0 + K\left(\frac{H_s(t) - H_c}{H_{ref}}\right)^n \quad \text{for} \quad H_s > H_c \tag{4.2}$$

$$c_e(t) = c_0 \quad \text{for} \quad H_s < H_c \tag{4.3}$$

where c_0 is a non-settling background concentration, and K is a re-suspension parameter that will in general depend on the substrate characteristics and the depth of the water column h i.e. it is location specific. Bed erodibility is described by Ravens (1997) as crucial for re-suspension modelling that is dependent on benthic composition. H_s is the significant wave height, while H_c is a critical wave height below which no re-suspension occurs, and H_{ref} is a reference wave height - we assume it to be equal to H_c. The exponent n describes the relationship between the wave induced bottom shear stress τ and the wave induced orbital velocity u. The shear stress is expected to scale

as $\tau \sim u^2$. For nearly monochromatic waves with a single dominant wave period, this suggests $n \approx 2$.

The background concentration c_0 was observed during long periods of little to no wave action. This persistent suspended sediment may be attributed to tiny inorganic micro-flocs and organic planktonic species whose rate of settlement is much lower than the rate ascribed to the majority of the particles in the water column.

Assuming that c_e is constant within the time interval Δt which is taken as 15 minutes in this study, integrating equation 4.1 over the time interval $(t, t + \Delta t)$ yields a difference equation

$$c(t + \Delta t) = c(t)e^{-w_s \Delta t/h} + c_e(t)\left(1 - e^{-w_s \Delta t/h}\right) \tag{4.4}$$

which can be used to predict the SSC concentration given the local wave characteristics and the parameters K, H_c and H_{ref}, w_s, and depth h.

The settling velocity w_s may depend on the SSC and particle size distribution (Luettich *et al.*, 1990). For example, following high wave events coarser material with a higher settling velocity may dominate the water column. Calm periods may result in a water column dominated by smaller particles with a lower settling velocity. One way of including the effect of this variation in average settling velocity is to assign a variable settling velocity dependent on each time interval's SSC,

$$w_s = w_0 \ (c/c_0 - 1)^{\alpha} \tag{4.5}$$

where w_0 represents a reference settling velocity, and α is a variable that controls the sensitivity of the settling velocity to SSC concentration.

Model parameters K, H_c and H_{ref} were optimised for each pole site to factor in the unique sediment composition there using the Microsoft Excel solver tool. K was constrained to an upper limit value of 125mg.ℓ^{-1}. This value was informed by the value used by Luettich *et al.* (1990) whose bottom material sediment size distribution was within the same order of magnitude as our study. Luettich describes K as a model parameter and it has been understood that this term indirectly accounts for bed erodibility. Settling velocities were constrained to the range 0.02 – 0.10 cm.s^{-1} based on the results obtained by Maine (2011) who analysed similar sediment samples collected from the nearby uMfolozi estuary.

4.4 Results

4.4.1 Overview

In this study we observed the diurnal wind pattern of low night-time speeds (typically < 4 m.s^{-1}) to high mid-day speeds (typically > 6 m.s^{-1}). This pattern is characteristic of Lake St Lucia. Wind directions regularly alternated between north/north-easterly to south to south-westerly. Night time winds were thermally driven land breezes predominantly originating from the west.

In April strong wind persisting for approximately twelve hour periods were repeatedly observed during the day. The third day of the study coincided with the passage of a south-easterly storm while the last two days were relatively calmer (refer to Figure 4.3).

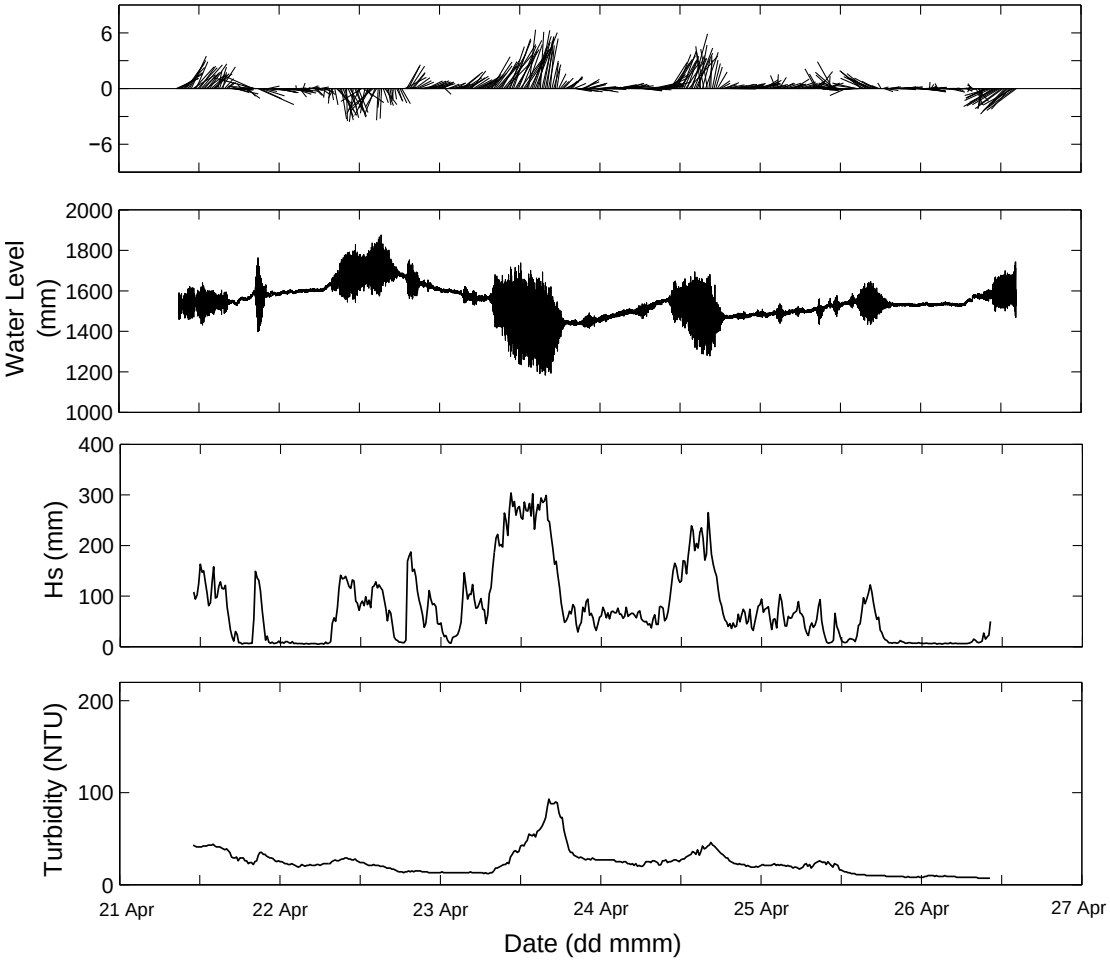

Figure 4.3: April pole station AP3 wind vector plot (top panel), water level time series (second panel), significant wave height time series (third panel) and turbidity time series (bottom panel).

In July a period of persistent wind lasting approximately 36 hours and varying in direction from north-easterly to north-westerly was observed on the second day. Wind directions were overall strongly aligned towards the northern and southern directions (refer to Figure 4.4).

Significant wave heights or wave energy measured over the course of the study increased almost immediately in response to changes in wind speed and direction. As

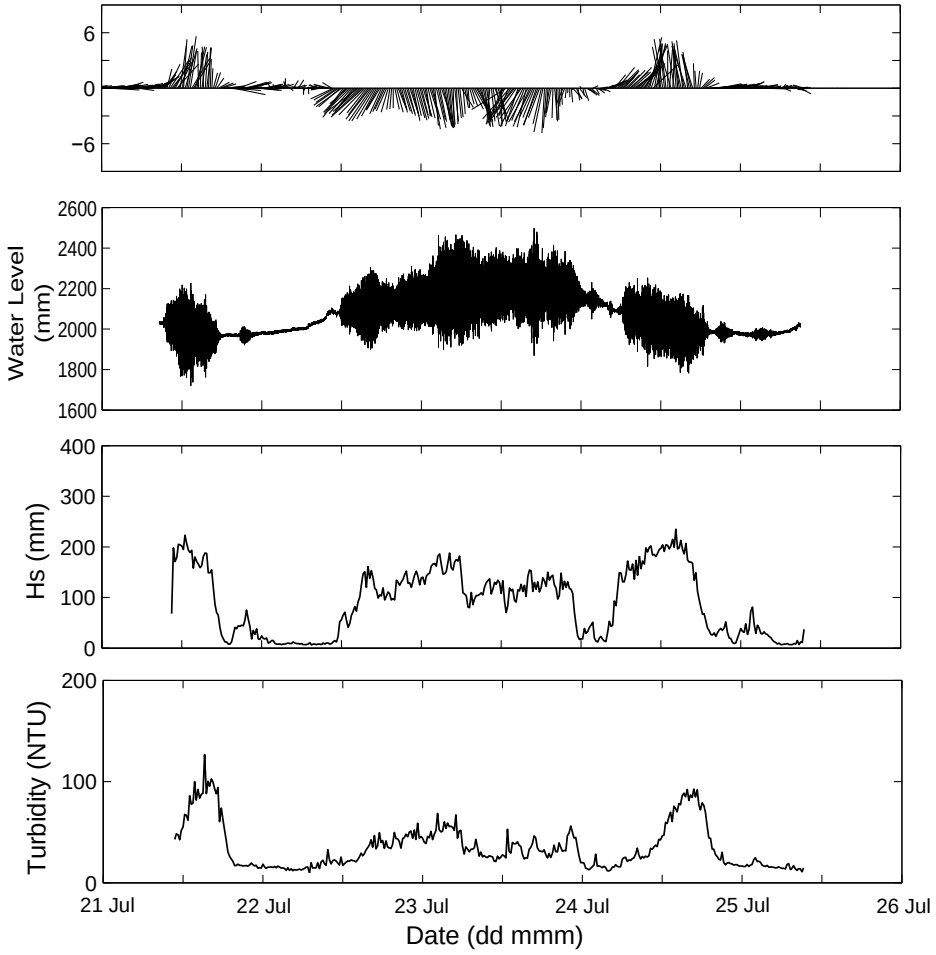

Figure 4.4: July pole station JP3 wind vector plot (top panel), water level time series (second panel), significant wave height time series (third panel) and turbidity time series (bottom panel). The water level, significant wave height and turbidity time series for JP0 closely resemble JP3 and have not been included.

expected high wind speeds acting in directions aligned with larger fetches resulted in more pronounced waves events and greater observed significant wave heights (see Figures 4.3, 4.4 and 4.5). The variation observed during the peak H_s events may be attributed to the effect of gusts and slight variations in wind speed and direction as outlined in our previous study (see Zikhali *et al.* (2014)). Water depths for each pole site changed in response to changes in wind direction with site JP3 having the greatest average depth (see Table 4.1).

In January measured wind speeds were high from mid-day of the first day into the night, only dying down during the middle of the second day. The daily alternation in direction was not apparent (refer to Figure 4.5).

Table 4.1: Range of depths observed during the course of the study

Pole station station	Avg depth range (mm)	Water level range (mm)
AP3	1410 – 1730	1180 – 1880
JP0	820 – 1070	660 – 1190
JP3	1850 – 2090	1720 – 2500
JAN3	740 – 970	620 – 1010

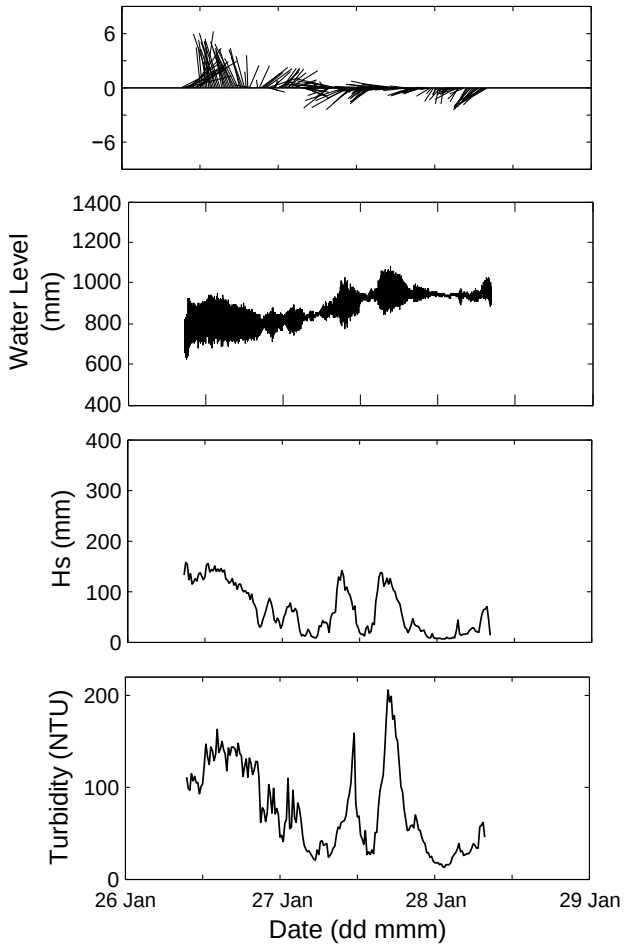

Figure 4.5: January pole station JAN3 wind vector plot (top panel), water level time series (second panel), significant wave height time series (third panel) and turbidity time series (bottom panel).

Bailey & Hamilton (1997) describes how re-suspension is a function of the bottom shear stress induced by fluid motion. Qian *et al.* (2011) and Brand *et al.* (2010) note how sediment re-suspension may be linked directly to wind speed, except where advective currents have a significant influence since waves and currents may sometimes develop independently. The relationship between turbidity and significant wave height measured at pole AP3 appears to be more weakly correlated than the relationship observed at positions JP0/JP3 and JAN3 (see Figures 4.3, 4.4 and 4.5).

In April a northerly high wind event that occurred on the second day caused a significant spike in measured turbidity levels. Peak H_s observed at site AP3 was just under 200 mm. Turbidity levels only rose above 100 NTU during a southerly storm event on the third day. This was attributed to a peak H_s of 300 mm at the time. A similar southerly high wind on the fourth day resulted in a lesser increase in turbidity, here H_s peaked at 250 mm. In July strong southerly winds resulted in rapid spikes in turbidity with peak H_s reaching 200 mm at site JP0 corresponding to a turbidity nearly 130 NTU. Similar northerly high winds caused peak H_s to reach 150 mm and resulted in gradual increases in turbidity.

The turbidity time series compiled in January for site JAN3 differed significantly from sites AP3 and JP3. Spikes in turbidity were observed for southerly wind directions as well as the north easterly to easterly directions. Peak H_s values were approximately 150 mm while turbidity rose above 170 NTU and peaked at 206 NTU.

A persistent layer of cohesive, fluid mud was identified over the deep muddy centre of the South Lake. This fluid mud layer was ranged between 0.5 – 0.8 m in depth at points T1 and T2 which were investigated in April (refer to Figure 4.1). Vertical turbidity-depth profiles for these regions were typically uniform but with a slight increase in turbidity with depth only observed on two occasions. Research conducted by Ross & Mehta (1989) suggests the presence of a stable lutocline may reduce mixing rates with the water column above.

Figure 4.6 shows a set of turbidity profiles compiled on the 22nd of April during relatively windy conditions. Here the average turbidity for all profiles was relatively higher than profiles compiled on the 21st of April, which experienced calmer wind conditions. A significant turbidity gradient of $\approx$ 20 NTU can be observed over a depth of 1 m at station AP2 on the 22nd. On the 22nd a gradient is observed at station AP2. This gradient was not observed on the 21st during calmer conditions at the same location. On the 21st a gradient was instead observed at station AP4. The gradient may be due to measurements taken during a significant change in wave activity resulting in a new equilibrium SSC. This transition would cause non-uniform mixing for only a short period following the change in wave activity. Qian *et al.* (2011) also observed a vertical SSC gradient which became more pronounced at higher wind (and hence wind-wave) conditions in their laboratory flume experiments.

Ross & Mehta (1989) and Wu *et al.* (2013) suggest that the energy required for turbulent mixing and uniform concentration over most of the water column is provided mainly by wind-driven wave activity. Despite the shifted mean the water column remained well mixed in most cases with a sudden turbidity gradient only consistently

observed near the lake bed.

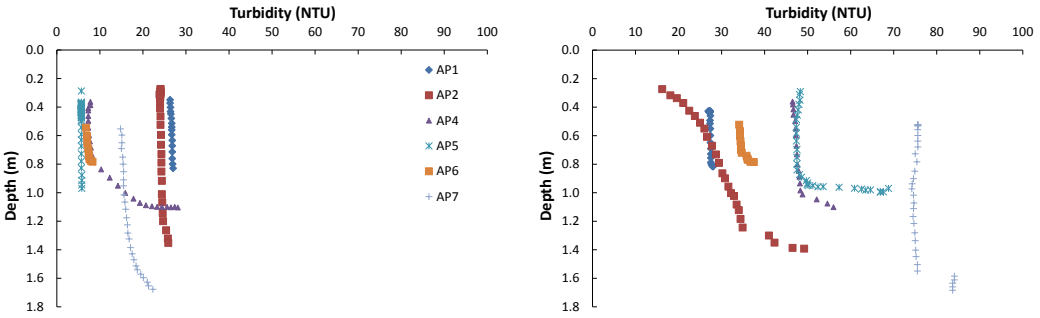

(a) (b)

Figure 4.6: Turbidity profiles taken at six positions within the sandy mud region of St Lucia's South Lake in April. Figure (a) shows those samples from the 21^{st} between the times 07:15 and 11:15 , while Figure (b) shows those readings which were compiled during relatively windier conditions on the 22^{nd} between 09:40 and 11:15.

4.4.2 Turbidity – SSC calibration

The advective current modelled in the study by Schoen *et al.* (2014) in South Lake was found to be low (typically < 0.2 m.s^{-1}). This finding supports the assumption that sediment entrained in the water column originates from the immediate surrounding or benthic layer below. Since the total surface area of South Lake is primarily made up of mud (refer to Figure 4.1) a sediment sample collected from the lake interior was deemed an appropriate representation of the majority of the sampling sites (see Table 4.2). The turbidity-to-SSC relationship established in our study was similar to the relationship derived by Cyrus (1988) although their ratio of NTU to SSC was almost 1:1. The relationship derived in our study was found to be 1 NTU for every 1.36 mg.ℓ^{-1} of suspended sediment (see Figure 4.7).

Table 4.2: Pole station sediment core sample size distributions

Sample site	**Sediment core D_{10} sizes (μm)**		**Sediment core D_{50} sizes (μm)**		**Sediment core D_{90} sizes (μm)**		**Clay %**	**Silt %**	**Sand %**	**Class**
	min	**max**	**min**	**max**	**min**	**max**				
AP3	54.4	139	277	303	529	591	0.300	8.10	91.6	Sand
JP0	6.90	13.7	219	227	415	424	1.90	22.1	76.0	Muddy sand
JP3	3.00	3.80	66.4	85.6	308	312	5.40	44.2	50.4	Sandy mud
JAN3	8.40	10.3	191	309	432	738	1.40	28.9	69.7	Muddy sand

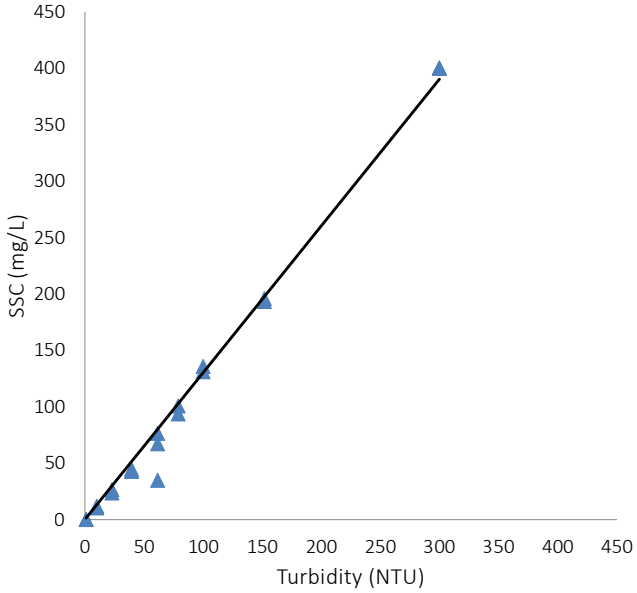

Figure 4.7: Turbidity versus SSC calibration results with a linear regression line. The sediment sample used was collected near pole station JP3 (see Fig 4.1).

The D_{50} particle size of the calibration material ranged from 11 to 14 μm. This particle size is similar to the D_{50} size of the suspended sediment analysed from water samples collected during April (see Table 4.3). The D_{50} size of the suspended sediment in these water samples typically ranged between 8 and 19 μm.

Table 4.3: Pole station suspended sediment sample size distributions

Sample site	**Sediment core D_{10} sizes (μm)**		**Sediment core D_{50} sizes (μm)**		**Sediment core D_{90} sizes (μm)**		**Clay %**	**Silt %**	**Sand %**
	min	**max**	**min**	**max**	**min**	**max**			
AP3	2.60	4.80	8.40	14.9	23.6	45.2	4.80	93.0	2.20
T1	1.50	3.40	5.70	10.6	12.8	33.5	7.40	90.4	2.20
T2	1.90	2.80	5.80	7.60	11.7	17.3	8.57	91.1	0.40

4.4.3 Model comparison with measured SSC

The Luettich *et al.* (1990) model was used to simulate sediment re-suspension using the observed H_s and h together with model parameters H_c, w_s and K. Observed turbidity was related to SSC by using the calibration curve in Figure 4.7. The observed SSC and

the modelled SSC were then compared.

Figure 4.8 shows time series of the observed SSC for each pole site. For all results a cross-correlation analysis revealed a delay between the occurrence of a change in wave action and a corresponding change in the turbidity (and hence the SSC) levels. This delay between wave event and change in SSC was found to average 15 minutes. Model accuracy varied with each sampling station. Using a constant settling velocity (Figure 4.8) the model tended to under-predict the SSC levels observed but followed the general trend in all cases. Peaks were well captured but in the case of JAN3, severe under-prediction was observed.

The parameters derived for each sample site set were optimized using the Excel solver tool. A comparison between this study's parameters and those derived by Luettich is shown in Table 4.4. Note that Luettich *et al.* (1990) determined acceptable parameter set combinations by identifying the values that resulted in Mean Square Errors (MSE) values that were within 30% of the lowest value identified. For this study only the range of values associated with the lowest identified error were selected. The range of our error parameters relates to the range observed between different pole stations.

A uniform settling velocity w_s for SSC below 400 mg.ℓ^{-1} is suggested by Ross & Mehta (1989) and our results appeared to reflect the observed settling rate well for SSC above 100 mg.ℓ^{-1}. However when concentration reached approximately 50 mg.ℓ^{01} we observed a decrease in the settling rate. The model did not capture this trend in most instances. The use of the dynamic settling velocity slightly improved the simulation of the reduced settling at low concentrations however the modelled results became highly irregular (in response to changing SSC) at higher concentrations. The benefit of using a variable w_s in this manner could not reconcile this occurrence at higher concentrations and the resulting modelled SSC was deemed unrealistic.

Table 4.4: Comparison between Luettich model parameters and the parameters derived for this study

Model parameters	**Luettich**	**Present study**
	range	**range**
$\mathbf{H_c}$ **(cm)**	0.00 – 17.0	4.80 – 13.1
w_s **(cm.s^{-1})**	0.02 – 0.03	0.02
n (unitless)	0.15 – 3.95	2.00
K (mg.ℓ^{-1})	0.00 – 125	44.1 – 61.8

The Luettich re-suspension model's performance varied with each pole station. Model performance was observed to improve as site mud content increased. The model exhibited the highest agreement index and efficiency index for site JP3, which also had the highest silt content. The bed composition of Lake Balaton where the Luettich *et al.* (1990) model was calibrated is in fact high in silt content. Table 4.5 contains an

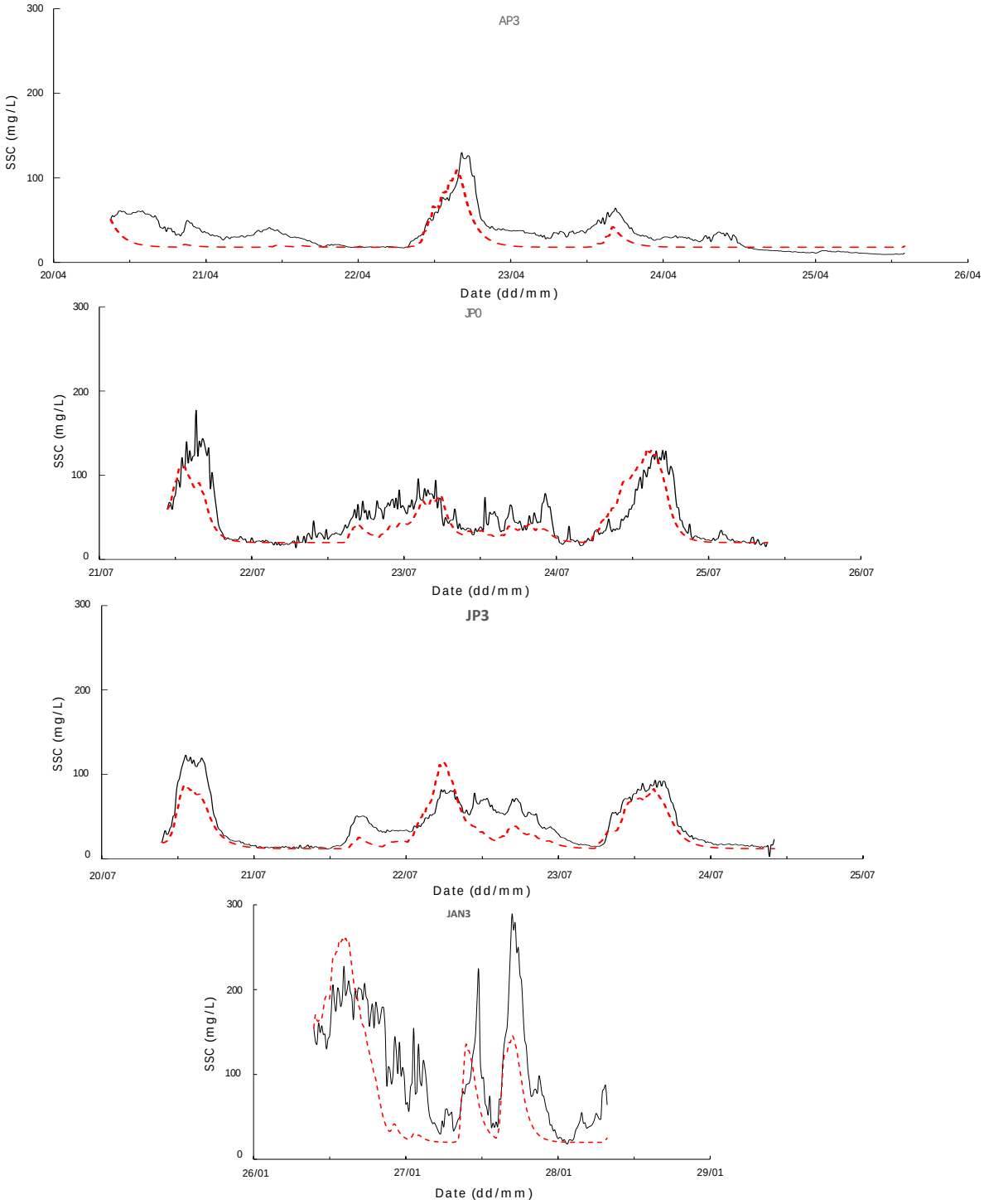

Figure 4.8: Observed SSC (—) and modelled SSC (- - -) for each sampling station set up in South Lake during the course of the study. Stations AP3 and JP0 were located in a predominantly sandy region,while station JAN3 had a muddier bed composition (refer to Figure 4.2). Station JP0 was located in the lake's relatively deeper, muddy central region.

analysis of the errors identified between the observed SSC and the modelled SSC.

Table 4.5: Error analysis of observed to modelled SSC. RMSE, observed and modelled mean values are in mg.ℓ^{-1}.

Pole station	Error parameter	value
AP3	Agreement index	0.57
	Efficiency index	0.35
	RMSE	16.0
	observed mean	33.0
	modelled mean	23.0
JP0	Agreement index	0.73
	Efficiency index	0.59
	RMSE	42.0
	observed mean	49.0
	modelled mean	41.0
JP3	Agreement index	0.73
	Efficiency index	0.61
	RMSE	17.0
	observed mean	42.0
	modelled mean	31.0
JAN3	Agreement index	0.65
	Efficiency index	0.26
	RMSE	56.0
	observed mean	106
	modelled mean	76.0

4.5 Discussion and Conclusions

This study measured changes in turbidity levels as a result of wave activity at various sites throughout Lake St. Lucia's South Lake basin where the bed substrate compositions differed for each site. The shallow lake provided the opportunity to assess the robustness of a depth averaged SSC model and observe whether calibrated model parameters should change with bed composition.

Our study concluded that a simple depth averaged re-suspension dynamics model can provide predictions of SSC in Lake St. Lucia's South Lake with varying degrees of accuracy. The Luettich *et al.* (1990) model simulates re-suspension dynamics best in areas with a fine, muddy sediment composition. Re-suspension dynamics differed both spatially and temporally necessitating unique model parameters for each pole position. Despite the differing benthic sediment classification of each pole station modelled peak SSC was consistently within comparable range of observed SSC. The model parameters adequately incorporated the differences in bed properties. Periods of under-prediction

appeared to be a common shortcoming at all pole stations and the resulting predictions of the suspended sediment dynamics varied in terms of predictive agreement and efficiency.

The re-suspension model displayed the highest discernible predictive performance at the site observed to have the greatest relative depth and finest bed sediment composition, site JP3 (see Table 4.5). The site where the model performed poorest, site AP3, consisted of a coarser sediment distribution with the lowest silt content and lowest average depth (see Table 4.1). The model frequently under predicted the SSC observed following an increased wave event. It was noted that the model was less sensitive to increases in H_s when H_s was low, resulting in no observable increases in SSC.

Sediment re-suspension events are limited by either input energy due to wave action or bed composition factors. Bed shear resistance is known to increase with layer depth, bed cohesiveness and structural integrity (Ross & Mehta, 1989). However the Luettich equation does not contain a term that considers limitations to re-suspension due to decreasing erosion rates. For an undisturbed bed initial re-suspension rates may be high only to decrease underlying layers with higher critical shear strength are exposed, reducing erosion rates (Aberle *et al.*, 2004). A 0.5 m thick fluid mud layer was visually identified and persistent over pole sites positioned in areas classified as muddy. Similar to the layer observed by Wu *et al.* (2013) in their study this layer was bonded weakly to the bed. Bed shear resistance was therefore expected to be low in these regions as described in Wu *et al.* (2013), while peak equilibrium SSC was expected to be high. This persistent layer was not observed near pole sites positioned in regions classified as sandy. The bed shear resistance in sandy regions was therefore expected to be relatively higher, and the re-suspension SSC was expected to reach a lower peak SSC during the highest wave events. It was expected that the muddier regions (poles AP3 and JP3) would generally experience higher turbidity levels than the sandier regions (poles JP0 and JAN3).

Peak turbidities measured in April and July were comparable to those measured in the study by Wu *et al.* (2013). Although this system is different from ours the trends observed were similar namely: short time intervals between increased wind-wave activity and re-suspension events, a rapid increase in SSC due to sensitivity to wave events and very short periods of high SSC followed by rapid deposition events. Measurements summarised in Figure 4.6 generally show no turbidity gradient with depth down to the region of the near-bed lutocline layer where a sudden increase in gradient occurred. However on two occasions a turbidity gradient was observed, at different pole sites for each day.

The delay in re-suspension compared to wave activity is partially attributable to the time taken for changes in equilibrium SSC to permeate to upper levels of the water column where the turbidity probe was positioned. When wave action died down the persistence of smaller particles may have caused turbidity readings to remain high even though larger particles may have already settled out. This may be associated with differing settling velocities of different sediment sizes.

The sediment type distribution reported by Fortuin (1992) (see also Perissinotto

et al., 2013, Fig 9.5) showed discrepancy from the results of our analysis. In general samples from the regions where we analysed D_{50} particles were either one class coarser or finer in comparison to those identified by Fortuin. MacKay *et al.* (2010) conducted multiple sediment distribution surveys in South Lake over the period of 2004 - 2008. A slight variation in the seasonal size distribution can be identified in their results although whether this is attributable to the drought conditions during this period of time is not certain. Similar studies in South Lake of sediment distribution over time suggest changes in sediment classification with time Pillay & Perissinotto (2008), which may explain discrepancies in the model's predictive ability. Changes in sediment composition would affect benthic erodibility and consequent re-suspension dynamics (Ravens, 1997).

No significant variation in SSC size distribution with depth was observed therefore a single settling velocity was initially applied to each pole site. Analysis of the collected turbidity data revealed increased settling fluxes immediately following high wave events. This effect was poorly emulated by a constant w_s. Attempts were made to improve the model by considering the observed difference in the rate of sediment re-suspension compared to the rate of settling (Equation 4.5). This led to the application of a variable settling velocity. The results did not significantly change the settling rate exhibited by the model. Sediment deposition is a complicated process that may be dependent on more factors than the suspended sediment concentration and the settling velocity. The work of Wu *et al.* (2013) utilised a deposition rate that incorporated particle inertia due to wave and current induced turbulence. This approach is physically justifiable and could be applied to improve predictive accuracy however it would add to the complexity of the model.

The flows measured in the study by Wu *et al.* (2013) averaged between 0.02 – 0.03 $m.s^{-1}$, an order of magnitude below the flows expected in South Lake based on the model of Schoen *et al.* (2014). Despite this difference re-suspension dynamics were well modelled in the muddy part of South Lake. Including the effect of horizontal advection may improve further model predictions however the significance of this improvement depends on the advection speed and prevalence throughout the lake.

This research provided evidence the sediment re-suspension dynamics in the shallow South Lake of St Lucia can be modelled effectively. Peak SSC levels are captured by the model and while lower wave events are not as consistently converted into increases in SSC, the model should still provide a general idea of SSC and turbidity conditions throughout the South Lake as varying substrate conditions are accounted for by the model parameters.

References

Aberle, J., Nikora, V., Walters, R. (2004). Effects of bed material properties on cohesive sediment erosion. Marine Geology. 207. 83–93.

Bailey, M.C. & Hamilton, D.P. (1997). Wind induced sediment resuspension: a lake-wide model. Ecological Modelling. 99. 217–228.

Brand, A., Lacy, J.R., Hsu, K., Hoover, D., Gladding, S., Stacey, M.T. (2010). Wind-enhanced resuspension in the shallow waters of South San Francisco Bay: Mechanisms and potential implications for cohesive sediment transport. Journal of Geophysical Research.115. 1–15.

Carrasco, N., Perissinotto, R., & Jones, S. (2013). Turbidity effects on feeding and mortality of the copepod Acartiella natalensis (Connell and Grindley, 1974) in the St. Lucia Estuary, South Africa. Journal of Experimental Marine Biology and Ecology. 446. 45–51.

Castaing, P. & Allen, G.P. (1981). Mechanism controlling seaward escape of suspended sediment from the Gironde: a macrotidal estuary in France. Marine Geology. 40. 101–118.

Cloern, J. (1987). Turbidity as a control on phytoplankton biomass and productivity in estuaries. Continental Shelf Research. 7. 1367–1381.

Cozar, A., Galvez, J.A., Hull, V., Garcia, C.M., Loiselle, S.A. (2005). Sediment resuspension by wind in a shallow lake of Esteros del Ibera (Argentina): a model based on turbidimetry. Ecological Modelling. 186. 63–76.

Cyrus, D.P. (1988). Turbidity and Other Physical Factors in Natal Estuarine Systems Part 2: Estuarine Lakes. Journal of Limnological Society of South Africa. 14. 72–81.

Cyrus D.P & Blaber S.J.M. (1988). The influence of turbidity on juvenile marine fishes in estuaries. Part 1: Field studies at Lake St Lucia on the Southeastern coast of Africa. In: Pringle, J.J. (2011). Wind induced sediment re-suspension in a shallow lake. South Africa: University of KwaZulu-Natal.

Das, B.M. (2010). Priniciples of geotechnical engineering: Seventh Edition. Stamford. Cengage Learning.

REFERENCES

Folk, R.L., (1954). The Distinction between Grain Size and Mineral Composition in Sedimentary-Rock Nomenclature. The Journal of Geology. 62. 4. 344–359.

Fortuin, H. H. G. (1992). Sediment Distribution Patterns in Lake St Lucia. CSIR Division of Earth, Marine & Atmospheric Science & Technology, Research Report 712.

Jin, K.R. & Ji, Z.G. (2001). Calibration and verification of a spectral wind-wave model for Lake Okeechobee. Ocean Engineering. 28. 571–584.

Lawrie, R.A. & Stretch, D.D. (2011a). Anthropogenic impacts on the water and salinity budgets of St Lucia estuarine lake in South Africa. Estuarine, Coastal and Shelf Science. 93, 58–67.

Lawrie, R.A. & Stretch, D.D. (2011b). Occurrence and persistence of water level/salinity states and the ecological impacts for St Lucia estuarine lake, South Africa. Estuarine, Coastal and Shelf Science. 95, 67–76.

Legates, D.R. & McCabe, G.J.Jr. (1999). Evaluating the use of "goodness-of-fit" measures in hydrological and hydroclimactic model validation. Water Resources Research. 35. 233–241.

Liu, J.H., Yang, S.L., Zhu, Q., Zhang,J. (2014). Control on suspended sediment concentration profiles in the shallow and turbid Yangtze Estuary. Continental Shelf Research. Article in press.

Luettich, R.A., Harleman, D.R.F., Somlydody, L. (1990). Dynamic behaviour of suspended sediment concentration in a shallow lake perturbed by episodic wind events. Limnology and Oceanography. 35. 1050–1067.

Mackay, F., Cyrus, D., Russell, K.-L. (2010). Macrobenthic invertebrate responses to prolonged drought in South Africa's largest estuarine lake complex. Estuarine, Coastal and Shelf Science. 86. 553–567.

Maine, C. (2011). The flocculation dynamics of cohesive sediments in the St Lucia and Mfolozi estuaries, South Africa. University of KwaZulu-Natal: South Africa.

Perissinotto, R., Stretch, DD, & Taylor, RH (eds), 2013. *Ecology and Conservation of Estuarine Ecosystems: Lake St. Lucia as a Global Model*. Cambridge University Press.

Pillay, D. & Perissinotto, R. (2008). The benthic macrofauna of the St. Lucia Estuary during the 2005 drought year. Estuarine, Coastal and Shelf Science. 77. 35–46.

Qian, J., Zheng, S., Wang, P., Wang, C. (2011). Experimental Study on Sediment Resuspension in Taihu Lake Under Different Hydrodynamic Disturbances. Journal of Hydrodynamics. 23(6). 825–833.

Ravens, T. (1997). Sediment Resuspension in Boston Harbor. Boston, United States of America: Massachusetts Institute of Technology.

Ross, M.A. & Mehta, A.J., (1989). On the Mechanics of Lutoclines and Fluid Mud. Journal of Coastal Research SE. 5. 51–62.

Schoen, J., Stretch, D.D. & Tirok, K., 2014. Wind-driven circulation in a shallow estuarine lake: St Lucia, South Africa. *Estuarine, Coastal and Shelf Science*. 146. 49–59.

Tirok, K. & Scharler, U.M. (2014). Influence of variable water depth and turbidity on microalgae production in a shallow estuarine lake system - a modelling study. Estuarine, Coastal and Shelf Science. 146. 111–127.

Wiberg, P.L. & Sherwood, C.R. (2008). Calculating wave-generated bottom orbital velocities from surface-wave parameters. Computers & Geosciences. 34. 1243–1262.

Wu, D. & Hua, Z. (2014). The effect of vegetation on sediment resuspension and phosphorus release under hydrodynamic disturbance in shallow lakes. Ecological Engineering. 69. 55–62.

Wu, T., Qin, B., Zhu, G., Zhu, M., Li, W., Luan, C. (2013). Modelling of turbidity dynamics caused by wind-induced waves and current in the Taihu Lake. International Journal of Sediment Research. 28. 139–148.

Zikhali, V., Tirok, K., Stretch, D. (2014). Wind driven waves in a shallow estuarine lake with muddy substrates: St Lucia, South Africa. Journal of Coastal Research. SI:70. 729–735.

Chapter 5

Synthesis

5.1 Wave modelling - summary of key results

The semi-empirical Young & Verhagen (1996) wave model was developed in Lake St George which is more uniform in depth and sandier in sediment composition. Young & Verhagen (1996) confirmed that wind-driven waves in shallow lakes develop similar to deep water waves except where depths are small relative to wavelength and waves may be classified as shallow water waves. These waves are limited in terms of the amount of energy and the wave height they can develop due to the limiting effect of the depth.

Our study concluded that the defining parameters for shallow water wave development in Lake St Lucia's South lake are: fetch distance, wind speed, wind direction relative to lake geometric properties and average depth over fetch. Lake St Lucia's hydrodynamic conditions are almost exclusively driven by the wind climate. For shallow lakes of this nature a thorough understanding of how wind develops and is distributed in the region is required (Allan & Kirk, 2000). The narrow band frequency distribution of 2 Hz for the waves observed in South Lake is largely due to the short fetch distances or to a low average wave age. Without tidal influences wind distributes water between the three basins and defines water levels, the wave spectrum and circulation patterns throughout South Lake (Schoen *et al.*, 2014).

The Young & Verhagen (1996) wave height model effectively predicted significant wave heights for varying fetch distances, depths and sediment composition conditions. Model predictions compared to observed H_S were scattered however a positive correlation persisted. The scatter was attributed to the variable wind speed and changes in wind directions. Small changes in wind direction together with South Lake's complex geometry led to large changes in fetch distance. This observation was most evident for high wind speeds when winds came from the northern constriction in the lake (for north/north-easterly winds) and over obstructions due to a small island to the south (for south/south-westerly winds).

Figure 5.1 and 5.2 show a comparison between the original results of Young & Verhagen (1996) and this study's . The upper and lower dashed lines of Figure 5.1 (a) describe the predicted non-dimensional wave energy for a non-dimensional depth of 0.1

and 0.2 respectively. For Figure 5.2 (a) the same is shown for non-dimensional depths 0.4 and 0.5. Once again the solid lines again represent the deep water asymptotic limit to wave energy described in Chapter 1.

A similar degree of scatter in observed wave energy can be seen in there results. The data subset derived for easterly/westerly waves, corresponding to shorter fetches than the northly/southerly waves, significantly deviated from the model trend contributing to the overall scatter. This increased scatter is present for both depth ranges in Figure 5.1 (a) and 5.2(a). The scatter observed in Figure 5.1 (b) and 5.2 (b) may therefore largely be attributed to waves developed over the shorter fetches, which in our study's case corresponded to north-easterly/south-westerly directions.

The Young & Verhagen model results did not show definitive instances of wave attenuation which could be attributed exclusively to sediment composition effects. The sediment composition of South Lake may not result in wave attenuation events for the wavelengths observed. Instances of depth limitation were only occasionally observed over the course of the study for the data collected. Where potential instances of depth limitation were observed the influence of sudden changes in fetch distance and variability in wind speed could not conclusively be ruled out.

The model was considered capable of simulating trends in significant wave heights development in Lake St Lucia South Lake despite the deficiencies discussed above. Therefore the model was used to provide input wave parameters for a simple sediment re-suspension dynamics model.

5.2 Sediment re-suspension - summary of key results

The Luettich *et al.* (1990) model was applied in Lake St Lucia to predict depth averaged SSC at pole stations distributed throughout South Lake. The model performed best when applied to muddy sites in the lake. The relationship between SSC and wave energy differed for each pole site as shown in Figure 5.3. This is in line with the observations of Cyrus (1988) whose study identified spatial variability in the lake's turbidity. In Figure 5.3 significant wave height is plotted against resulting SSC for each pole station. The re-suspension dynamic observed can be divided into two trends similar to the water level-NTU hysteris curve described for the Big Kuonamka River by Tananaev & Debolskiy (2014). Their study noted that the temporal correlation between turbidity peaks with water level peaks suggests a limit to the sediment re-suspended under hydrodynamic action. The shape and peak SSC of the trends observed in our study may therefore indicate the value of this limit for similar regions in Lake St Lucia.

The highest SSC in 5.3 (a) and (b) describes the upper trend which corresponds to sediment settling following a period of high wave activity. The bed sediment surrounding station AP3 and JP0 sites has the highest sand content at 92% and 76% respectively. During a sediment settling phase following an energetic wave event SSC remains high due to the abundance of entrained fine particles. These fine particles have a lower settling velocity than heavier sediment particles which require more wave energy to remain in suspension. Even with a low significant wave height these smaller

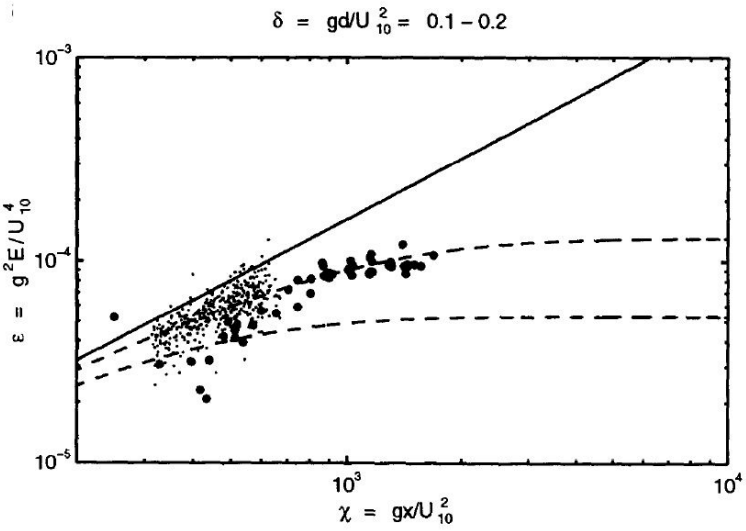

(a)

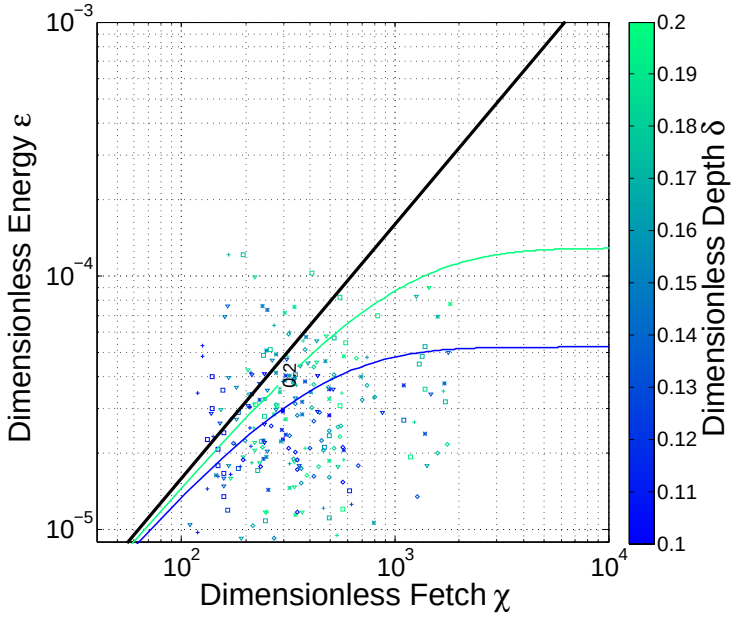

(b)

Figure 5.1: Comparison of the non-dimensional scatter plots for depths (δ) 0.1 - 0.2 of observed energy (ε) versus fetch (χ).(a) Results from the study by Young & Verhagen (1996), where the northerly/southerly wind direction waves are shown as large dots ($\bullet$) and the easterly/westerly waves are shown as small points ($\cdot$). (b) depicts the results of the current study where waves were not distinguished according to wind direction

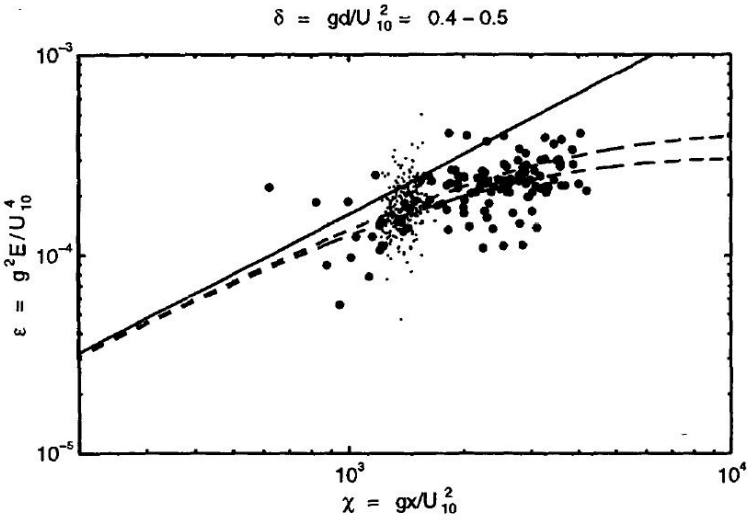

(a)

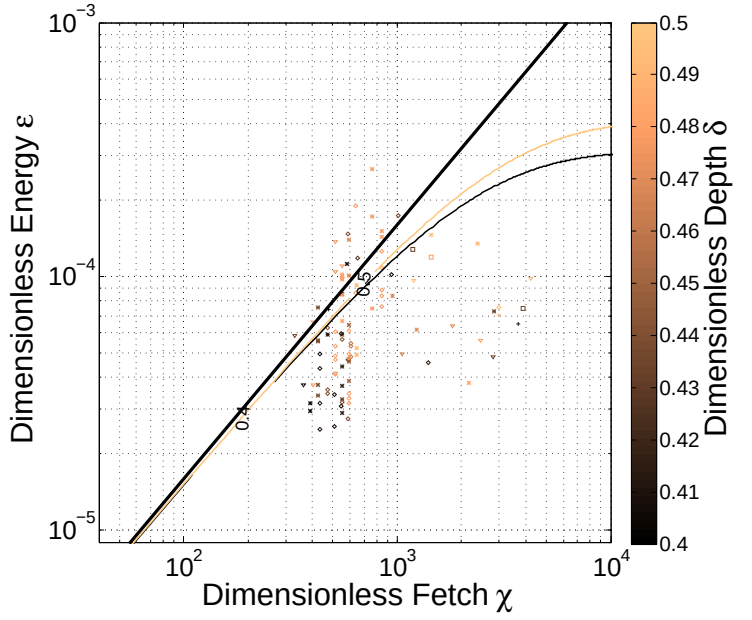

(b)

Figure 5.2: Comparison of the non-dimensional scatter plots for depths (δ) 0.4 - 0.5 of observed energy (ε) versus fetch (χ) taken from (a) Young & Verhagen (1996), where the northerly/southerly wind direction waves are shown as large dots ($\bullet$) and the easterly/westerly waves are shown as small points ($\cdot$). (b) depicts the results of the current study where waves were not distinguished according to wind direction.

particles can be kept in suspension resulting in a high SSC as observed in the results of the study by Qian *et al.* (2011).

The lower trend consisting of lower SSC for the range of H_s corresponds to the sediment re-suspension following a calm period. Here low significant wave heights are unable to overcome the shear resistance of the bed and transfer particles within the lutocline layer into overlying water column. As wave heights increase more excess shear energy is available and re-suspension events increase. This results in minimal initial sediment re-suspension rates and SSC levels which only gradually increase.

Plots (c) and (d) are derived from observations made at pole stations JP3 and JAN3 which have a finer bed sediment distribution. The relationship between H_s and SSC observed at these sites has a less defined upper and lower trend in SSC perhaps due to the entrained sediment being finer and more easily kept in suspension by low wave heights.

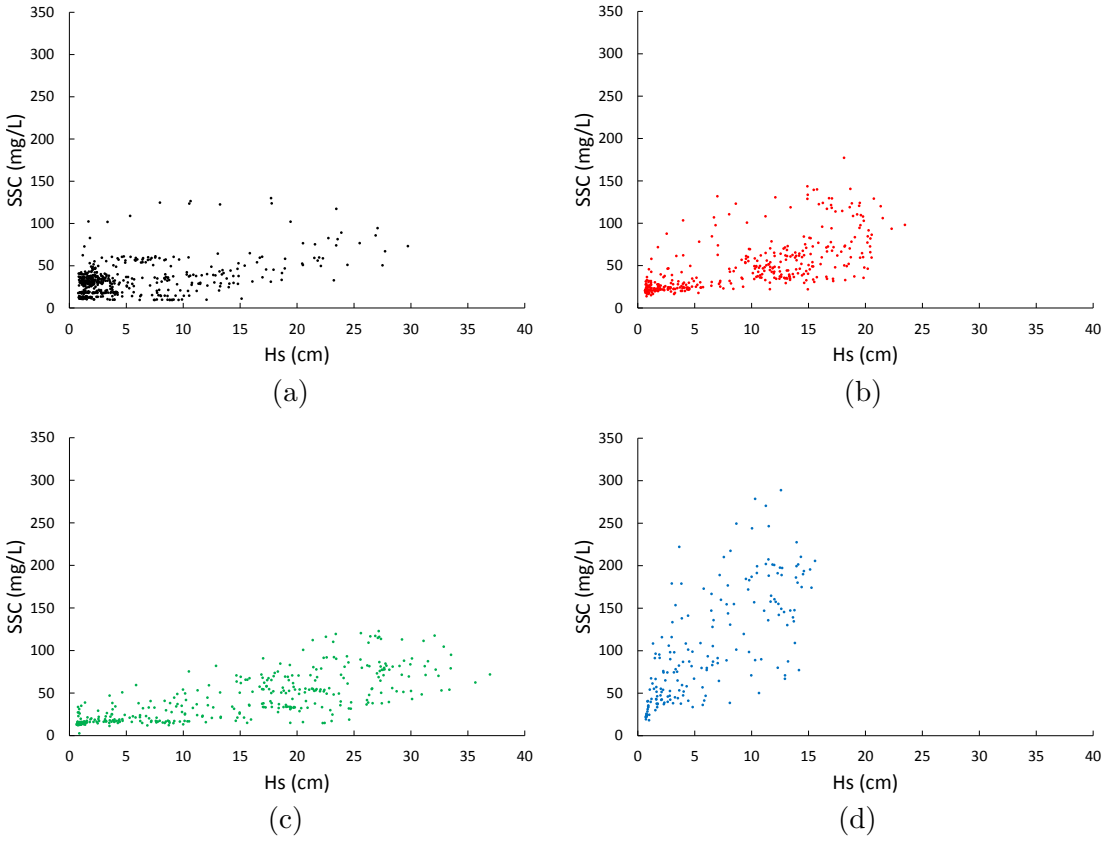

Figure 5.3: Observed H_s plotted against observed SSC. The re-suspension relationship at site AP3 is shown in (a), JP0 in (b), JP3 in (c) and JAN3 in (d).

Under southerly winds the turbidity and SSC was consistently higher at all pole stations relative to northerly wind conditions. A southerly wind usually resulted in

higher significant wave heights leading to higher re-suspension rates and more sediment entrainment.

5.3 Wave and SSC modelling combined

Significant wave heights derived using the Young & Verhagen model can be used as inputs to a calibrated Luettich model to simulate the suspended sediment concentration levels within South Lake (see Figure 5.4). The results of our analysis varied as the accuracy of the wave prediction model adversely affected the SSC model's predictive performance.

Side by side error analysis results reveal that the model performs poorly when using Young & Verhagen H_s input values compared to using observed H_s in all cases except JAN3. For JAN3 the agreement index in Table 5.1 is shown to improve by almost 0.2 for the Young & Verhagen modelled values while efficiency improves by almost 0.5.

Table 5.1: Error analysis of observed to modelled SSC where Young & Verhagen significant wave heights were used as input wave parameters. RMSE, observed mean and model mean values are in mg.ℓ^{-1}.

Pole station	Error parameter	Y & V Model value	Original Model value
AP3	Agreement index	0.44	0.57
	Efficiency index	-0.15	0.35
	RMSE	39.0	16.0
	observed mean	33.0	33.0
	model mean	20.4	23.0
JP0	Agreement index	0.62	0.73
	Efficiency index	-1.71	0.59
	RMSE	27.0	42.0
	observed mean	49.0	49.0
	model mean	57.0	41.0
JP3	Agreement index	0.58	0.73
	Efficiency index	0.08	0.61
	RMSE	27.0	17.0
	observed mean	42.0	42.0
	model mean	23.0	31.0
JAN3	Agreement index	0.82	0.65
	Efficiency index	0.73	0.26
	RMSE	205.0	56.0
	observed mean	106	106
	model mean	92.0	76.0

The Young & Verhagen model has therefore provided a simulation of the H_s trends

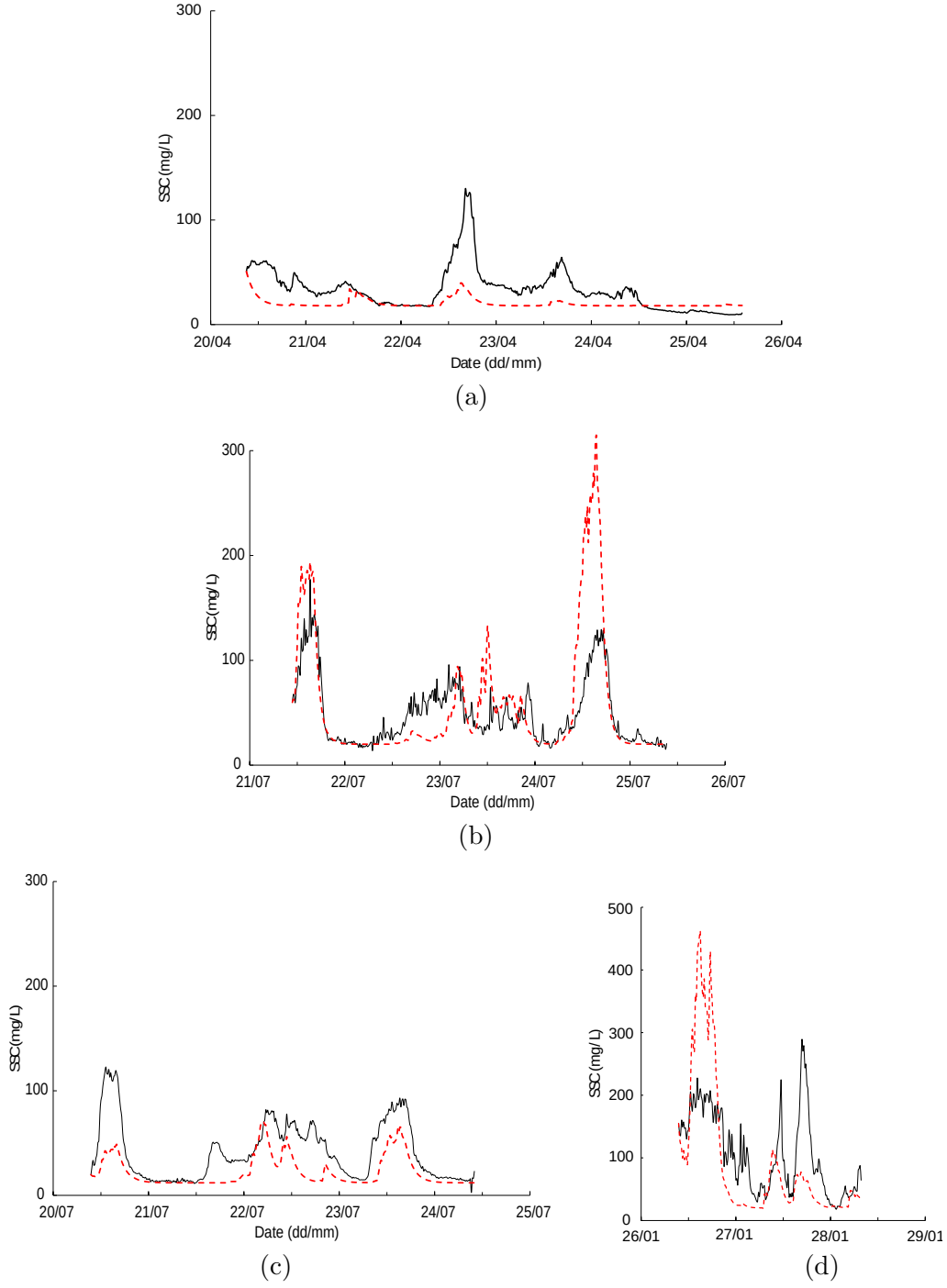

Figure 5.4: Observed SSC (–) and modelled SSC (- -), where the H*s* parameter for the model was derived using the Young and Verhagen model. Diagram (a) describes station AP3, (b) and describes station JP0, these poles were located in relatively sandier regions. Diagram (c) describes station JP3 which was situated in the muddy central region and (d) describes station JAN3, located near station JP0.

and parameters that effectively predict the range of SSC normally observed in Lake St Lucia in select circumstances. Predicted SSC was in the same order of magnitude for all pole station cases. The discrepancy between observed and predicted results suggests that the model only be applied where general SSC trends or average turbidities with an error range of about 300 mg.ℓ or 220 NTU are required. Using the model to predict turbidities with greater accuracy requires further refinement of the model parameters. The results of the combined model may therefore be improved by refining the predictive ability of the Young & Verhagen model and by conducting a detailed bathymetric survey to accurately define the range of bed sediment compositions in South Lake and how these changes with time.

5.3.1 South Lake ecological impacts

Wind-waves are known to affect the vertical distribution of buoyant phytoplankton in shallow lakes by reducing their numbers during high wave events (Cao *et al.*, 2006). Cyanobacteria in particular, which can be detrimental to biodiversity and dissolved oxygen levels (Svircev *et al.*, 2014; Sukenik *et al.*, 1998), can be stimulated to bloom by winds as low as 2 m.s^{-1} and wave heights of 0.04 m. A further increase of approximately 25% in wind speed and wave height may then cause blooms to disappear from the surface into the depths (Cao *et al.*, 2006). This behaviour highlights the extreme sensitivity of the ecology to wind driven wave conditions. The waves observed in our study generally ranged between 0.2 – 0.3 m suggesting that wave activity alone is unlikely to be conducive to a major bloom due the water column being kept well mixed.

High turbidity levels can affect freshwater fish colonies in a variety of ways as described by Berli *et al.* (2014). In turbid conditions fish swimming ability may be impaired and physiological indicators of acute stress have been identified. On the other hand reduced visibility provided by turbid conditions can allow zooplankton to co-exist in large numbers with predatory fish thereby promoting biodiversity (Carrasco *et al.*, 2013). The larval development of fish who use the St Lucia estuarine environment is also affected. Larval density has been observed to increase with higher turbidities (Cyrus, 1988; Harris & Cyrus, 1995).

The SSC observed during our study generally ranged between 20 to 150 mg.ℓ^{-1}. In January values of up to 300 mg.ℓ^{-1} were observed during the course of a storm. The findings of Carrasco *et al.* (2013) indicate that turbidities from 500–1000 NTU can significantly affect copepod mortality rates depending on exposure time. These turbidities correspond to SSC of 706 mg.ℓ^{-1} to 1413 mg.ℓ^{-1}. Turbidity is unlikely to to reach or be maintained at such high magnitudes in the deeper parts of the lake or at shallow depths. Our findings suggest that peak SSC is only maintained for short periods of time even when influenced by high wind-wave events.

Frequent changes in SSC may have an adverse effect on the microbiology of the shallow lake. High variability in turbidity may reduce seasonal microalgae production at low mean turbidities or increase production when mean turbidity is high Tirok & Scharler (2014). A model investigating the effects of variable water levels and turbidities

developed by Tirok & Scharler (2014) describes how turbidities above 150 NTU significantly reduce light availability in Lake St Lucia. Their mathematical model describes how depth and turbidity influence long term biomass production. Their results indicate that at greater depths log mean turbidities above 40 NTU resulted in reduced net biomass production. In our study all observed average SSC were above 30 mg.ℓ^{-1} which corresponds to turbidities above 21 NTU. The highest average turbidity of 75 NTU (or 106 mg.ℓ^{-1}) was observed at site JAN3. This suggests the majority of the sites investigated provide an environment that does not significantly limit light penetration. Pole site JAN3 is close in proximity to site JP0 however there is a significant difference in their average turbidities (JP0 displayed an average turbidity of 35 NTU). This difference exists despite similar wave activity and peak H_s for both sites.

References

Allan, J.C. & Kirk, R.M. (2000). Wind wave characteristics at Lake Dunstan, South Island, New Zealand. New Zealand Journal of Marine and Freshwater Research. 34:4. 573–591.

Berli, B.I., Gilbert, M.J.H., Ralph, A.L., Tierney, K.B., Burkhardt-Holm, P. (2014). Acute exposure to a common suspended sediment affects the swimming performance and physiology of juvenile salmonids. Comparative Biochemistry and Physiology, Part A. 176. 1–10.

Cao, H-S., Kong, F-X., Luo, L-C., Shi, X-L., Yang, Z., Zhang, X-F., Tao, Y. (2006). Effects of Wind-Induced Waves on Vertical Phytoplankton Distribution and Surface Blooms of Microcystis aeruginosa in Lake Taihu. Journal of Freshwater Ecology. 21:2. 231–238.

Carrasco, N.K., Perissinotto, R., Jones, S. (2013). Turbidity effects on feeding and mortality of the copepod Acartiella natalensis (Connell and Grindley, 1974) in the St Lucia Estuary, South Africa. Journal of Experimental Marine Biology and Ecology. 446. 45–51.

Cyrus, D.P. (1988). Turbidity and Other Physical Factors in Natal Estuarine Systems Part 2: Estuarine Lakes. Journal of Limnological Society of South Africa. 14. 72–81.

Harris, S.A. & Cyrus, D.P. (1995). Occurrence of fish larvae in the St Lucia Estuary, KwaZulu-Natal, South Africa. South African Journal of Marine Science. 16:1. 333–350.

Luettich, R.A., Harleman, D.R.F., Somlydody, L. (1990). Dynamic behaviour of suspended sediment concentration in a shallow lake perturbed by episodic wind events. 35. 1050–1067

Tananaev, N.I. & Debolskiy, M.V. (2014). Turbidity observations in sediment flux studies: Examples from Russian rivers in cold environments. Geomorphology. 218. 63–71.

Qian, J., Zheng, S., Wang, P., Wang, C. (2011). Experimental Study on Sediment Resuspension in Taihu Lake Under Different Hydrodynamic Disturbances. Journal of Hydrodynamics. 23(6). 825–833.

Svircev, Z.B., Tokodi, N., Drobac, D., Codd, G.A. (2014). Cyanobacteria in aquatic ecosystems in Serbia: effects on water quality, human health and biodiversity. Systematics and Biodiversity. 12:3. 261–270.

Schoen, J., Stretch, D.D. & Tirok, K. (2014). Wind-driven circulation in a shallow estuarine lake: St Lucia, South Africa. *Estuarine, Coastal and Shelf Science*, submitted.

Sukenik, A., Rosin, C., Porat, R., Teltsch, B., Banker, R., Carmeli, S. (1998). Toxins from Cyanobacteria and their Potential Impact on Water Quality of Lake Kinneret, Israel. Israel Journal of Plant Sciences. 46:2. 109–115.

Tirok, K. & Scharler, U.M. (2014). Influence of variable water depth and turbidity on microalgae production in a shallow estuarine lake system - a modelling study. Estuarine, Coastal and Shelf Science. 146. 111–127.

Young, I. & Verhagen, L. (1996). The growth of fetch-limited waves in water of finite depth. Part 1: The total energy and peak frequency. Coastal Enineering, 29, 57–48.

Chapter 6

Conclusion and Recommendations

6.1 Introduction

The aim of this study was to characterise wind-driven waves in a shallow lake and assess the applicability of a wave prediction model alongside a re-suspension dynamics model. This chapter describes how this aim was achieved by summarising the work described in the preceding chapters according to the research questions outlined in Chapter 1.

6.2 Research answers

What are the factors affecting wave development in the simple shallow lake estuarine environment of Lake St Lucia South Lake?

The characteristics of wind-driven waves measured in South Lake are described in Chapter 3. The shallow lake waves were fetch distance and depth defined with significant wave heights consistently increasing with fetch regardless of sediment composition.

Although instances of depth limitation were identified these instances were not frequently observed. The effect of the irregular geometry of the lake was seen to influence wave development whenever a sudden change in wind direction occurred.

Can the wave spectrum of a shallow lake with variable substrate composition be simulated using a simple semi-empirical wave model?

This study found that the Young & Verhagen (1996) simple semi-empirical wave prediction model could be used to predict the wave climate provided that the wind and fetch were accurately defined, as described in Chapter 3.

The variable substrate did not appear to affect model performance significantly while sudden changes in wind speed, direction and fetch distance negatively impacted model accuracy.

Can a simple semi-empirical wave model be used to identify instances of wave attenuation in a shallow lake?

In Chapter 3 it is described how wave attenuation was identified in some instances however no definitive conclusion could be drawn due to the large amount of scatter observed in the results. Changes in substrate composition with fetch further added uncertainty to the results.

Can the sediment re-suspension and settling dynamics of a shallow lake with muddy substrate composition be modelled using a depth-averaged suspended sediment concentration model?

The re-suspension dynamics at the case study site were reasonably well-predicted by the Luettich model as described in Chapter 4. The model was observed to perform best where the depth was high and benthic sediment was composed of fine silt and clay material.

What effect do wave characteristics have on the biological functioning of a shallow lake estuarine environment?

In Chapter 5 it was concluded that high turbidity levels (described in Chapter 4) driven by wind-wave activity (described in Chapter 3) were likely to have adversely affected higher trophic levels of the South Lake ecology. Pelagic microalgae growth in deep water conditions may be less severely affected than benthic microalgae growth.

6.3 Recommendations for future research

This study found that the Young and Verhagen wave prediction model could provide reasonable predictions of the wave energy for the Luettich sediment re-suspension dynamics model. This result allows for the prediction of the suspended sediment concentrations using only wind speed, direction and bathymetric properties as input variables. The model could be improved by further investigating the wind field that governs the wave dynamics of Lake St Lucia.

The calibration of the Luettich model could be improved by performing a detailed bathymetric survey to determine the range of depths and the bed composition in Lake St Lucia on a finer, more detailed scale.